

THE ADAPTATION OF DUNES TO CHANGES IN RIVER FLOW

Reesink A.J.H.^(1,2,3,4), Parsons D.R.⁽¹⁾, Ashworth P.J.⁽²⁾, Best J.L.^(3,5), Hardy R.J.⁽⁶⁾, Murphy B.J.⁽¹⁾,
M^cLelland, S.J.⁽¹⁾, Unsworth C.⁽⁷⁾

¹ *School of Environment and Earth Science (Geography), University of Hull, Hull, HU6 7RX, UK*

² *Division of Geography and Geology, School of Environment and Technology, University of Brighton, Brighton, Sussex, BN2 4GJ, UK*

³ *Department of Geology, University of Illinois at Urbana-Champaign, 1301 W. Green St., Urbana, IL, 61801, USA*

⁴ *now at: Lancing College, Lancing, BN15 0RW, UK. Email: ajhr@lancing.org.uk*

⁵ *Departments of Geography and GIS, Mechanical Science and Engineering and Ven Te Chow Hydrosystems Laboratory, University of Illinois at Urbana-Champaign, 1301 W. Green St., Urbana, IL, 61801, USA,*

⁶ *Department of Geography, Durham University, Durham, DH1 3LE, UK*

⁷ *Department of Geography, University of Exeter, Exeter, EX4 4RJ, UK*

Keywords: dunes; floods, hysteresis; bedforms; ripples; bedform superimposition; sediment transport

ABSTRACT

The dunes that cover the beds of most alluvial channels change in size and shape over time and in space, which in turn affects the flow and sediment-transport dynamics of the river. However, both the precise mechanisms of such adaptation of dunes, and the hydraulic variables that control these processes, remain inadequately understood. This paper provides an overview of the processes involved in the maintenance and adaptation of dunes, provides new tools for the analysis of dune dynamics, and applies these to a series of bespoke experiments.

Dunes that grow compete for space, and dunes that decay need to shed excess sediment. Therefore, dune adaptation necessarily involves the redistribution of sediment over and among dunes. The details of sediment redistribution are not captured by mean geometric parameters such as dune height and wavelength. Therefore, new analyses of dune kinematics, bed-elevation distributions, and dune deformation are presented herein that aid the identification and analysis of dune dynamics.

Dune adaptation is often described as a morphological response to changes in water depth at a rate that depends on sediment mobility, which itself is a product of flow depth and velocity. However, depth and velocity are out-of-phase during the passage of flood waves, and they vary spatially across rivers from the thalweg to bar tops, and downstream along the river profile. In order to improve our understanding of the hydraulic controls on dune morphology and kinematics, a series of experiments was performed to investigate the response of dunes in fully-mobile sand ($D_{50} = 240\mu\text{m}$) to changes in flow depth and velocity.

The experimental results illustrate that water depth and flow velocity have separate effects on the processes that control dune adaptation, and that the crests and troughs of dunes do not respond simultaneously to changes in flow. Trough scour increases with flow velocity, but superelevation of the dune crests appear to show only a weak relation with flow depth. Flattening-out of dune crests is related to decreasing depth and increasing flow velocity. Bedform superimposition, a key feature of bedform kinematics, was associated with increased flow depth, but was also systematically associated with local increases in the crest-to-crest distance following the dissipation of an upstream

52 dune. Thus, local flow-form interactions have a significant effect on the manner in which sediment is
53 redistributed over and among dunes. The splitting of dunes decreased in the downstream direction
54 along the length of the flume, illustrating that the dunes continue to interact even after dune height
55 has stabilised. Other processes, such as differential migration and dune merging, are ubiquitous
56 during all flow conditions. These varied responses support the notion that the processes of dune
57 adaptation vary over time and in space.

58

59 Analysis of dune deformation through examination of the residuals of cross-correlations between
60 successive dune profiles illustrates that local sources and sinks of sediment exist within mobile dune
61 fields. These findings highlight that dune adaptation to changes in flow is a dynamic response
62 involving multiple interconnected dunes. The redistribution of sediment that is required for dunes to
63 change shape and adapt to new conditions is expected to be an important cause of variability in
64 sediment transport. These detailed analyses and findings provide a foundation for further study of
65 dune dynamics in different environments on Earth as well as other planetary bodies.

66

67 INTRODUCTION

68

69 Dunes are the most prominent and dynamic bedforms in alluvial channels. Dune growth and decay
70 affect flood height, flood-wave shape, and flood duration because dunes are a first order control on
71 the form roughness and resistance of river beds (Simons and Richardson 1966; Van Rijn, 1984; 1993;
72 Julien *et al.*, 2002; Warmink *et al.*, 2013). Coherent flow structures generated by dunes dictate the
73 vertical exchange of momentum and sediment in the flow, which affects the dissipation of energy
74 within the river as well as sediment budgets and bank erosion (Bennett and Best, 1995; Best,
75 2005a,b). Dune growth during flood events can even affect infrastructure, such as bridge
76 foundations and tunnels below the river bed (Amsler and García, 1997). Moreover, dune dynamics
77 affect sediment transport dynamics (Kleinhans *et al.*, 2007; Frings and Kleinhans, 2008), the
78 development of cross-strata (Kleinhans, 2004, Reesink and Bridge, 2007, 2009, 2011), the
79 preservation of sedimentary structures (Paola and Borgman, 1991; Leclair and Bridge, 2001;
80 Jerolmack and Mohrig, 2005; Reesink *et al.*, 2015), and the vertical and along-stream sediment
81 grading of bed sediment that affects the concavity of the river profile (Hoey and Ferguson, 1994;
82 Blom *et al.*, 2003, 2006). Thus, the dynamic development of dunes needs to be understood to
83 explain morphodynamic behaviour of river beds at a wide range of scales.

84

85 Dune development is controlled by the ‘morphodynamic’ feedback between the flow, sediment
86 transport, and dune forms (e.g. Leeder, 1983; Best, 1993, 1996; Bridge, 1993; Carling *et al.*, 2000;
87 Church and Ferguson, 2015). Whereas significant advances have been made recently in
88 quantification of flow over dunes through detailed measurements (Nelson *et al.*, 1993; Bennett and
89 Best, 1995; Best *et al.*, 2010; Unsworth *et al.*, in press.) and numerical models (e.g. Omidyeganeh
90 and Piomelli, 2011, 2013a,b; Naqshband *et al.*, 2014a; Schmeckle, 2014, 2015), comparatively little
91 is known about the processes of erosion and deposition that control how and why dunes change
92 their shape as they migrate. The first objective of this study is therefore to investigate
93 experimentally how dune geometries respond to changes in flow for a range of shallow,
94 unidirectional flow conditions.

95

96 Dunes continuously *deform* as they migrate, even in conditions where statistical descriptors of the
97 dune population have converged and the reach-averaged bed shear stress is constant (McElroy and
98 Mohrig, 2009). In addition to such steady-state deformation, dunes also *adapt* to changes in flow.
99 The adaptation of dunes is a response to both temporal changes in flow during floods (unsteady
100 flow; e.g. Allen, 1973, 1974, 1982; Julien and Klaassen, 1995; Wilbers and Ten Brinke, 2003) and to
101 spatial changes in flow related to channel form (non-uniform flow; e.g. Jackson, 1975, 1976;
102 Nittrouer *et al.*, 2008; Reesink *et al.*, 2015). The distinction between deformation (not specific to

103 disequilibrium) and adaptation (a consequence of disequilibrium conditions) is maintained herein.
104 The physical processes that control the deformation and adaptation of dunes are not necessarily
105 different, but will vary in magnitude and frequency (Kleinhans *et al.*, 2007; McElroy and Mohrig,
106 2009; Martin and Jerolmack, 2013). Precisely how the magnitude of these processes is linked to their
107 hydraulic controls is at present not adequately constrained. The second objective of this study is
108 therefore to investigate how the processes that control the development of dune shape vary in
109 response to changes in depth-averaged flow parameters, such as flow depth and velocity.

110
111 Recent advances in bathymetric survey techniques illustrate that dune geometries and dynamics
112 vary greatly across bars and channels (Parsons *et al.*, 2005; Nittrouer *et al.*, 2008; Claude *et al.*, 2012;
113 Rodrigues *et al.*, 2015; Almeida *et al.*, 2016), and even at close proximity within a single, stabilised
114 river (Kleinhans *et al.*, 2007; Frings and Kleinhans, 2008). In spite of such variation, dunes in river
115 channels are often assumed to follow the same predictive models (e.g. Giri and Shimizu, 2006;
116 Paarlberg *et al.*, 2009; Nabi *et al.*, 2013, 2015). Dunes are also often compared between different
117 environments, such as rivers, estuaries, shallow seas, deserts (Kocurek and Ewing, 2005), and even
118 other planets (e.g. Cutts and Smith, 1973; Diniega *et al.*, 2016) and asteroids (Thomas *et al.*, 2015).
119 However, no comprehensive conceptual framework is currently available to identify and interpret
120 differences in the development and ‘behaviour’ of dunes in these contrasting environments. There is
121 a distinct possibility that different processes may lead to similar sand bed morphologies (equifinality)
122 and that multiple processes are involved in bedform maintenance and evolution at any one time
123 (multiplicity; Schumm, 1998; Kleinhans *et al.*, 2017). The final objective of the present paper is
124 therefore to test new analytical tools for analysis of the development of dune shape.

125
126 To begin to investigate the dynamic changes in dune geometry (first objective) and the processes
127 that cause them (second objective) by means of a number of new analytical tools (third objective), a
128 series of physical experiments are presented herein that aim to monitor the response of mobile sand
129 dunes in shallow, unidirectional flows to changes in flow depth (depth 0.17-0.25 m) and velocity
130 (0.46-0.66 m s⁻¹). The dynamics observed in the experiments are unlikely to represent the dynamics
131 of dunes in deep water (depth-independent behaviour, c.f. Flemming and Bartholomä, 2012), multi-
132 directional flows, or air. However, the theory and methods of the present study provide the
133 foundation that is necessary for future investigations of dune dynamics in contrasting environments.
134 The key aspects of dune morphology, sediment transport, and flow that underpin the analysis are
135 discussed below.

136
137

138 **BACKGROUND**

139

140 *Morphology: adaptation and equilibrium*

141 The definition of an equilibrium dune form fundamentally underpins our ability to predict bed
142 roughness (Van Rijn, 1984; 1993). Past studies systematically emphasise that dune geometry is the
143 product of a hydrodynamic dependency between dune form and the co-evolving flow field (see
144 overviews in Bennett and Best, 1995, Best, 2005a; Coleman and Nikora, 2011). Dune height and
145 wavelength are often assumed to scale with flow depth in rivers (Yalin, 1964; Ashley, 1990; Bradley
146 and Venditti, 2017) and each dune is dynamically linked to its up- and down- stream counterparts
147 (Best, 2005a; Schatz and Herrmann, 2006; Reesink and Bridge, 2009; Unsworth *et al.*, in press). Such
148 dependencies strongly imply that dune size can be predicted for rivers (Ashley, 1990; Allen, 1982;
149 Naqshband *et al.*, 2014b; Bradley and Venditti, 2017).

150

151 However, determining an equilibrium dune shape is difficult because natural dune populations
152 contain a range of sizes and shapes (Nordin, 1971; Paola and Borgman, 1991; Leclair, 2002). The
153 difficulties in defining dune ‘equilibrium’ have led to fundamental disagreements about the relative

154 importance of i) steady-state variability inherent to stable dune populations (Nordin, 1971; Jackson
155 1976; Rubin and McCulloch, 1980; Paola and Borgman, 1991; Parsons *et al.*, 2005) and ii) the
156 inheritance of dune morphology from past flow events (Allen, 1982; Allen and Collinson, 1974), as
157 controls on dune geometry.

158
159 Indeed, variability in dune shape may be caused by *deformation* of dunes as they migrate. Variability
160 in shape is deemed intrinsic to sediment transport over dunes, and hence expected to also occur
161 under equilibrium conditions (Venditti *et al.*, 2005a; McElroy and Mohrig, 2009). Additional
162 variability is introduced by the *adaptation* of dunes to changes in flow. Dune adaptation is
163 ubiquitous because river flow is characteristically both unsteady and non-uniform at the temporal
164 and spatial scales that are needed for dunes to reach equilibrium (Allen, 1978; Allen and Friend,
165 1976; Ten Brinke *et al.*, 1999; Kleinhans *et al.*, 2007). Further deviations from a simplified
166 relationship between dune geometry and depth can be attributed to variables such as changes in
167 viscosity, turbulence, and the shape of the velocity profile (e.g. Smith and Ettema, 1997), grain-size
168 sorting and the development of coarse-grained pavements (Tuijnder *et al.*, 2009; Rodrigues *et al.*,
169 2015), sediment bypassing and suspension (Nittrouer *et al.*, 2008; Szupiany *et al.*, 2012; Naqshband
170 *et al.*, 2014a), Froude number and water surface interactions (Naqshband *et al.*, 2014b), suspension
171 of clays (Wan and Wang, 1994; Baas and Best, 2002; Baas *et al.*, 2009, 2016), and cohesion of the
172 bed (Schindler *et al.*, 2015; Malarkey *et al.*, 2015; Parsons *et al.*, 2016).

173
174 It is important to stress that dunes are also rarely in equilibrium because any geometric change
175 requires both time and sufficient sediment transport. The delayed development of dunes relative to
176 their formative flow is known as dune hysteresis (e.g. Allen, 1974; Ten Brinke *et al.*, 1999; Kleinhans
177 *et al.*, 2007; Martin and Jerolmack, 2013). Although such hysteresis is commonly described as a
178 temporal lag between bed morphology and the formative flow, other studies suggest that the
179 processes of growth and decay of dunes differ (e.g. Martin and Jerolmack, 2013). There is, therefore,
180 a need to identify precisely which processes are involved in the growth and decay of dunes, and at
181 what spatial and temporal scales these processes operate.

182
183 The rate at which dunes adapt to new flow conditions depends on the rate of sediment transport
184 and is considered to decrease non-linearly towards an equilibrium state (Paarlberg *et al.*, 2010;
185 Martin and Jerolmack, 2013). Convergence of parameters such as bedform height, wavelength,
186 steepness (e.g. Van der Mark *et al.*, 2008) and 'deformation flux', which describes deformation as a
187 proportion of downstream migration, may provide practical solutions for the definition of an
188 equilibrium form (McElroy and Mohrig, 2009). However, simplifications of dune morphology to
189 mean geometric parameters introduce a loss of information, and remain strictly valid for the
190 conditions for which they were tested until the underlying processes are fully understood.

191
192 *Sediment transport: dispersal of sediment over and between dunes*

193 Dunes compete for space while migrating. In order for one dune to grow, another must reduce in
194 size to accommodate this growth. Significant dune adaptation requires dunes to be added to, or
195 removed from, the dune field, and this occurs through merging or splitting of dunes (Fig. 1A-B;
196 Raudkivi and Witte, 1990; Coleman and Melville, 1994). The new merged or split dunes have height-
197 length ratios that differ significantly from their surrounding dunes (Fig. 1A-B, Flemming, 2000), which
198 leads to spatial unevenness in the flow-form feedback processes within the dune field. As a
199 consequence, the competition for space between dunes leads to the redistribution of sediment
200 across the dune field. Any study of dune adaptation is therefore a study of sediment dispersal over
201 and between dunes (Reesink *et al.*, 2016).

202
203 The redistribution of sediment over and among dunes is controlled by multiple sediment transport
204 processes (Fig. 1C-I). Bedload sediment can be suspended temporarily and therefore bypass one, or

205 several, dunes (Fig. 1C; e.g. Jopling, 1965; Allen, 1982; Kostaschuk, *et al.*, 2009; Naqshband *et al.*,
206 2014a). Sediment transport paths are likely to vary in response to spatial and temporal variability in
207 velocity and turbulence over dune fields (Allen, 1982; Reesink and Bridge, 2009). Indeed, field
208 measurements of dune form and suspension of sand across bars and through bends show that rates
209 of sediment bypass can vary across successive dunes (Nittrouer *et al.*, 2008; Szupiany *et al.*, 2012).
210 Sediment dispersal can also be achieved through differential migration of dunes (Fig. 1D; Martin and
211 Jerolmack, 2013), or by the introduction and storage of sediment by differential scour (Fig. 1E;
212 Gabel, 1993; Leclair, 2002). Modification of dune shape may involve superimposition of bedforms
213 (Fig. 1F; Best, 2005a; Fernandez *et al.*, 2006), which has also been described as the mechanism by
214 which sediment moves over host dunes (Ditchfield and Best, 1992; Venditti, 2005a). Bedform
215 superimposition is also essential for the onset of bedform splitting (Gabel, 1993; Warmink *et al.*,
216 2014) and essential to the through-passing of superimposed bedforms (Fig. 1G; Venditti *et al.*,
217 2005b). The relative role of through-passing of smaller bedforms, as opposed to bypassing of
218 suspended sediment, is likely a function of grain size and transport stage. The volume of sediment
219 transported by dune migration can also be modified by changing dune geometry from a triangular
220 profile to a humpback profile (Saunderson and Lockett, 1983; Carling *et al.*, 2000; Reesink and
221 Bridge, 2009). The magnitude of sediment transport is, however, not captured fully by simple
222 metrics such as bedform height and wavelength, and is problematic in cases where changes in dune
223 form and size indicate significant transfer of sediment between dunes (Ten Brinke *et al.*, 1999;
224 McElroy and Mohrig, 2009). Both bedform superimposition and changes in dune geometry affect the
225 flow field over dunes (Fig. 1H; Best and Kostaschuk, 2002; Fernandez *et al.*, 2006; Reesink and
226 Bridge, 2009; Kwoil *et al.*, 2016; Lefebvre *et al.*, 2016) and hence the sediment transport dynamics
227 (Reesink and Bridge, 2009). Finally, sediment can be dispersed in the cross-stream direction (Fig. 1I;
228 Allen, 1982), which is likely more pronounced when dunes have more variable three-dimensional
229 geometries (Parsons *et al.*, 2005). This can create strong local flow structures and affect the
230 direction gravity-controlled grainflows, especially in cases where larger scale secondary circulation
231 may exist in addition to the flow over the dunes.

232
233 The relative importance of the multitude of processes that disperse sediment over and among dunes
234 changes in response to both grain size and bed shear stress (McElroy and Mohrig, 2009; Martin and
235 Jerolmack, 2013; Venditti *et al.*, 2016; Bradley and Venditti, 2017). Dune development is known to
236 vary significantly over time, in space, and between different reaches of river channels (e.g. Kleinhans
237 *et al.*, 2007), with the instabilities in dune patterns being transferred through the dune field by
238 means of flow-form feedback processes, which are expected to gradually dissipate (Werner and
239 Kocurek, 1997, 1999; Venditti *et al.*, 2005b; Ewing and Kocurek, 2010). However, the relative
240 importance of individual processes remains poorly constrained. To begin to address these issues, the
241 present paper investigates the response of dunes to changes in flow using new methods for the
242 visualisation of dune deformation, which provides objective evidence for the analysis of the
243 processes that control dune development (Reesink *et al.*, 2016).

244
245 *Flow: depth and water surface slope*
246 The best-known hydrodynamic association between dune form and flow is the positive correlation
247 between dune height and wavelength with water depth (Yalin, 1964; Ashley, 1990; Van Rijn, 1993;
248 Bradley and Venditti, 2017). Despite the spatial complexity of dune fields in rivers and the systematic
249 deviations from a simple correlation discussed earlier, the dependency of dunes on flow depth is at
250 least, in part, supported by observations of dune growth during floods and by the presence of large
251 dunes in large rivers (Amsler and Garcia, 1997; Julien and Klaassen, 1995; Wilbers and Ten Brinke,
252 1999; Best *et al.*, 2007). It is therefore clear that the depth of the formative flow is an important
253 control on dune adaptation.

254

255 In most rivers, flow depth is correlated with discharge at individual gauging stations through rating
256 curves, although the flow depth for a given discharge depends on the form roughness generated by
257 the bed and bar forms (Simons and Richardson, 1966; Dawdy, 1965; Garcia, 2006; Van Rijn, 1993).
258 Because dune adaptation changes bed roughness, dune height and flow depth are not strictly
259 independent during the passage of floods. In flume experiments and numerical predictions of dune
260 adaptation, flow depth, water surface slope, flow velocity, and discharge are often considered to be
261 interdependent (Paarlberg *et al.*, 2009; Martin and Jerolmack, 2013; Warmink *et al.*, 2014; Nabi *et*
262 *al.*, 2015). Such simplifications are indeed justified for a considerable range of scales (Schumm,
263 1977).

264
265 However, the relative magnitudes of flow depth and water surface slope vary systematically in rivers
266 at the spatial scale of the dune wavelength, and at the temporal scale required for dunes to migrate
267 this distance. Temporally, the water depth and water-surface slope that drive sediment transport
268 are out-of-phase during the passage of significant flood waves (Fig. 2). This is well-known for
269 pronounced, symmetrical waves in simple tidal systems (Fig. 2A; e.g. Martinus and Van den Berg,
270 2011; Dalrymple *et al.*, 2015), but is equally valid for non-tidal rivers in which flood waves are
271 superimposed on the water-surface gradient that is associated with the baseflow discharge (Fig. 2B).
272 The loop-like relation between water-surface slope and water depth (Fig. 2C) is significant even for
273 relatively large rivers and floods that last for weeks, such as in the Mississippi (Fig. 3). The
274 characteristic asymmetry of fluvial flood waves is clearly indicated by the larger number of days with
275 decreased water-surface slopes (Fig. 3). Thus, not only are the relative magnitudes of slope and
276 depth variable, but the relative duration of specific combinations of slope and depth will vary
277 between environments, floods, and different locations along and within a river.

278
279 The relative magnitudes of flow depth and water-surface slope also vary spatially. Changes in flow
280 depth and water surface slope between the thalweg and bar tops (Fig. 4A) result in variations in
281 tractive forces, sediment transport, erosion and deposition (Bridge, 1993), similar to that which has
282 been extensively investigated for pools and riffles (Carling, 1991; Sear, 1996; Milan *et al.*, 2001). At a
283 larger spatial scale across drainage basins, flow depth and water-surface slope vary between shallow
284 and steep upstream channels, to deeper and lower-gradient lowland channels, to tidal channels (Fig.
285 4B; Leopold and Maddock, 1953). The consequences of such systematic variability in hydraulic
286 variables for dune development remain poorly understood. The experiments conducted herein were
287 thus designed to investigate the roles of water depth and velocity on the kinematics of dune
288 development.

289

290

291 **METHODS**

292

293 In order to investigate the response of dunes to changes in water depth and flow velocity, a series of
294 controlled experiments was designed in which measurements of flow velocity, water depth, and
295 bathymetry were made in an experimental flume with a fully-mobile sediment bed. A series of novel
296 analyses was developed to determine how the imposed changes in flow conditions affected the
297 dune morphology and sediment redistribution. The experiments and analytical techniques are
298 discussed below.

299

300 **Experimental set-up and measurements**

301 In the present experiments, fully-mobile dunes were developed in sand with median grain size of
302 240 μ m in a sediment-recirculating flume that was 16m long, 2m wide and 0.5m deep, which was
303 constructed in the Total Environment Simulator in The Deep Facility at the University of Hull, UK (Fig.
304 5). A flow baffle was placed at the upstream end of the channel to dissipate turbulence generated by
305 the pumps and inlet to the flume (Fig. 5A). Additional slurry pumps were installed to prevent the

306 build-up of sand within the recirculating loop (Fig. 5A). Flow depth and discharge were increased and
307 decreased both independently and in unison (Table 1) within the known limits of dune stability (cf.
308 Van den Berg and Van Gelder, 1993). The stage-discharge combinations correspond to Froude
309 numbers ranging from 0.3 to 0.5 (Table 1) and overlap conditions used by Unsworth *et al.* (in press).
310 This set-up produced bedforms that could be compared directly to those found in shallow natural
311 sand-bed rivers without using any scaling relationships (Fig. 5B).

312

313 Changes in discharge were achieved using the flume pump, whilst water depth was changed via
314 rapid addition or subtraction of water from the flume, into a set of ten Intermediary Bulk Containers
315 (IBC's) of 1000 litres each. Water surface slope, flow velocity, bed shear stress, sediment transport,
316 and Froude number responded to the changes in depth and discharge. The imposed changes in flow
317 depth and velocity occurred faster (1-5 minutes depending on water volume) than the repetition
318 rate of the bathymetric profiles (5 minutes). The changes in morphology are thus considered to be
319 stepwise in comparison to the bathymetric profiles. A total of 24 stage-discharge combinations were
320 explored (Table 1), resulting in 23 adaptations (Table 2). Each stage-discharge combination was
321 maintained for as long as the dunes that existed at the start of the new conditions took to migrate
322 through the flume test section. The replacement of the existing bed by a new dune bed that
323 developed entirely under the new conditions took between 1.5 to 3 hours across all experiments.

324

325 Flow velocity, water level, and bathymetry were measured throughout the experiments in a 5 m long
326 test section located in the centre of the flume (Fig. 5A). The depth-averaged flow velocity was
327 measured using a set of four fixed Nortek acoustic Doppler velocimeters (ADV's) sampling at a rate
328 of 25 Hz. The measurements were made at 40% of the water depth from the bed at 4 locations in
329 the test section, which, assuming the law-of-the-wall, provides a measure of the average flow
330 velocity. Discharge was monitored using a built-in electromagnetic pipe gauge (Euromag MC106C).
331 The development the dune morphology and bed elevation were measured along the centreline of
332 the flume at 5 minute intervals using an AQUAscat™ acoustic backscatter probe operating at 4 MHz,
333 which was mounted on a Stebon™ 6m robotic traverse. The vertical and horizontal resolution of the
334 acoustic backscatter measurements were 2.5 and 5 mm respectively, with the bed elevation being
335 determined from the maximum amplitude of the acoustic backscatter return. Noise and spikes in the
336 elevation data were filtered out using visually established elevation threshold values and a median
337 filter. The data were then averaged to provide a value that corresponded to the experimental
338 intervals, which are used herein as an average value only. Water depth and water-surface slope
339 were measured along the test section at 2Hz using 7 wave height probes (HR Wallingford WG8 Twin-
340 wire wave rod system) that were spaced 1 m apart and located 0.75 m from the centreline of the
341 flume in order to enable the robotic carriage to move (Fig. 5A). The bed elevation measurements
342 were corrected relative to the still-water level. The flume was drained slowly to minimise
343 deformation of the sand bed after every four experimental runs in order to allow detailed scanning
344 of the sand bed with a Terrestrial Laser Scanner to millimetre resolution (Leica ScanStation2).

345

346 **Analysis of dune adaptation**

347 In order to investigate the adaptation of dunes to imposed changes in flow, the analysis presented
348 herein focusses on the dune longitudinal profiles from 0.5 hours prior to the imposed changes, until
349 1 hour after the imposed change (Fig. 6A; 9). Most of the dunes migrated out of the 5 m long test
350 section within this period. Therefore, beyond 1 hour, the dunes in the test section represented new
351 dunes that developed downstream from the flow baffle under the new flow conditions, and do not
352 represent dunes that were adapting to the imposed conditions. In addition, as the effect of any
353 change in flow depth and velocity on dune morphology can be expected to decrease over time
354 (Allen, 1974, 1982; Martin and Jerolmack, 2013), restricting the time period of the analysis allows
355 focus on the role of the imposed flow changes and decreases inclusion of the role of variability that
356 is inherent to the dune population.

357
358 Mean heights and wavelengths of the primary dunes were defined based on their crossing of the
359 mean bed elevation that was calculated over the entire length of the test section (Table 1; cf. Van
360 der Mark *et al.*, 2008). Although this objective method introduces some superimposed bedforms
361 into the bedform distribution, visual inspection indicated that the method closely matches a
362 subjective classification of the dunes. However, the simplification of dune shape to parameters such
363 as dune wavelength and height does not provide sufficient evidence to interpret the processes that
364 control dune deformation and adaptation. Therefore, changes in bed topography are further
365 analysed in several complementary ways, which are discussed below: i) dune kinematics, including
366 the gain and loss of the number of dunes, and bedform superimposition, ii) temporal changes in the
367 bed elevation distribution, and iii) deformation of dunes as revealed by the residuals of cross-
368 correlated profiles (Reesink *et al.*, 2016)

369 *Dune Kinematics: gain and loss of dunes, unstable dune patterns, and superimposed bedforms*

370 Kinematic analysis refers to the identification of interactions between dunes, which includes key
371 adaptation processes such as bedform splitting, merging, overtaking, and dissipation (Gabel, 1993;
372 Warmink, 2014). In order to analyse such dune kinematics, primary dunes first need to be defined
373 and distinguished from other bedforms, and then dunes need to be traced across successive profiles
374 in a systematic way in order to identify their appearance and disappearance.

375
376
377 Primary dunes can be distinguished from smaller-scale superimposed, ephemeral, incipient and
378 decayed bedforms by considering their temporal development as well as their geometries (cf. Gabel,
379 1993; Bridge, 2003, p. 86-87). Herein, a primary dune is defined as an asymmetrical bedform >0.05
380 m high and >0.2 m long that can be traced across at least three longitudinal profiles (herein >15
381 minutes). These criteria do not aim to distinguish between ripples and dunes, nor provide a method
382 for the identification of the presence or absence of ripples (for ripple stability, see Kleinhans *et al.*,
383 2017). Inherent to the practical definition used herein is a lower limit where the temporal and/or
384 spatial resolution is insufficient for unambiguous identification of dunes. This practical limit
385 constrains a class of spatially aliased, ephemeral, and/or superimposed bedforms that presents a
386 useful indicator of the inability of the dune field to achieve a stable configuration by itself.

387
388 For the kinematic analysis, dunes were traced between profiles by outlining the positions of both the
389 crests and troughs of the bedforms (Fig. 6B; cf. Allen and Friend, 1976, their fig. 1B). The
390 interpretation of kinematic behaviour is acknowledged to be sensitive to the spatio-temporal
391 resolution of the measurements. For example, what appears to be the dissipation of a dune may be
392 dune overtaking revealed in a higher temporal resolution dataset. Therefore, kinematic interactions
393 are herein simplified to: i) a gain in the number of dunes; ii) a loss in the number of dunes. The gain
394 of dunes includes dune splitting, emergence of dunes, and the amalgamation of incipient forms that
395 were not classified as dunes. Loss of dunes includes merging of dunes, overtaking of dunes, and
396 dying out (Raudkivi and Witte, 1990; Gabel, 1993; Coleman and Melville, 1994; Warmink *et al.*, 2014;
397 Warmink, 2014). Significant spatial aliasing between profiles is interpreted as a separate case of
398 interest: iii) instability within the dune pattern. Finally, the analysis of consecutive dune profiles
399 makes it possible to make simple observations of temporal changes in dune geometry, including iv)
400 the presence of trains of superimposed bedforms, and v) dune flattening.

401 *Bed elevation distributions*

402 Bed elevation distributions, as opposed to dune height distributions, can be considered to represent
403 the average bed morphology (e.g. Coleman *et al.*, 2011). The use of the bed elevation distribution is
404 independent from the identification and classification of bedforms, which is beneficial in cases with
405 complex and changing bed morphology. Herein, the bed elevation distribution is calculated for
406 individual profiles and plotted over time as a grey-scale, relative to the median elevation (Fig. 6C).

408 The temporal change in bed elevation distribution visualises changes in the mean bed form. In
409 particular, superelevation of the bedform crest, where the top of a dune builds higher into the flow,
410 and increased trough scour (e.g. Gabel, 1993) are readily visualised by widening of the distribution
411 towards the top and/or bottom (Fig. 6C).

412

413 *Dune migration and deformation*

414 Recent work illustrates how the motion of bedload sediment transport over dune-covered river beds
415 can be split, by means of cross-correlation, into two components: dune migration and dune
416 deformation (McElroy and Mohrig, 2009; Reesink *et al.*, 2016). In the present analysis, the migration
417 of dunes is removed by shifting the longitudinal bed profiles according to the first downstream
418 cross-correlation maximum (Fig. 7A; cf. McElroy and Mohrig, 2009). The cross-correlation shift is
419 indicated by the blanking at the left side of the dune profiles and indicates the dune ‘translation’, or
420 migration. The residuals of the cross-correlation illustrate spatial patterns in the deformation of the
421 dunes: localised loss and gain of sediment within the mobile dune field (Fig. 7B). Plotting the
422 deformation component for consecutive profiles thus visualises changes in spatial dune deformation
423 over time (Fig. 7C) and allows the identification of persistent sources and sinks of sediment within
424 the mobile dune field (Reesink *et al.*, 2016). The visualization displays a complex pattern of
425 deformation that requires further interpretation. Zones that are characterised by a dominant trend
426 in deformation can be seen, such as that outlined in Figure 7C. Alternatively, geomorphically
427 distinguishable elements, such as lee slopes, can be traced between profiles, and the loss or gain of
428 sediment from these elements over time can be interpreted (Fig. 7C; red and blue lines). The
429 hypothesis proposed herein is that these deformation patterns can be used as signatures for local
430 dune adaptation processes, such as acceleration, deceleration, growth and decay (Fig. 7D). Processes
431 such as bedform superimposition are likely associated with specific trends in the gain (blue) or loss
432 (red) of sediment from their host dunes, resulting in patterns that can be analysed and classified
433 (Fig. 7D). The analysis used herein is simplified after McElroy and Mohrig (2009) and does not
434 present cross-correlation decay coefficients, deformation half-times, and deformation ratios, which
435 proved less meaningful for the experimental results. This difference may be attributed to factors
436 such as the result of limitations imposed by shorter profile length, different sampling interval times,
437 higher mobility of the finer grain size, greater three-dimensional dune geometries, and the
438 abundance of superimposed bedforms in the present experiments. In addition, the methods of
439 McElroy and Mohrig (2009) are developed to quantify dune deformation in stable dune fields, and
440 not for the analysis of distinctly unstable dune patterns and adaptation of dunes to changes in flow.

441

442

443 **RESULTS**

444

445 The bed elevation measurements of dune geometries and the laser scans of the bed at selected
446 stage-discharge combinations (Fig. 8) illustrate that the size and geometry of the dunes varied
447 between different flow conditions (Table 1). Water-surface slope (Table 1) was found to vary greatly
448 in response to local dune morphology, and the times and distances required to establish reliable
449 water-surface slopes exceeded those involved in the response of individual dunes to changes in flow.
450 Overall, mean dune height in the experiments was ~0.1 m, and varied between ~0.05 m in the
451 shallowest water depths to ~0.19 m in the greatest water depths. Superimposed bedforms were less
452 common at higher flow velocities and lower water depths, and thus higher bed shear stresses. The
453 largest dunes were found in deeper water and under higher shear stresses, in contrast to the smaller
454 dunes in lower water depths and velocities (cf. Ashley, 1990; Van Rijn, 1993; Naqshband *et al.*
455 2014b; Bradley and Venditti, 2017). It is therefore expected that specific processes of deformation
456 and adaptation of dunes (Fig. 1) were significantly enhanced or reduced by the imposed changes in
457 flow depth and velocity, which was the aim of varying the flow stage in the experiments.

458

459 **Patterns in dune shape: bedform superimposition, flattening, and unstable dune pattern**

460 The general trends in the bed morphology described above were complicated by significant
461 variability in dune morphology and large numbers of superimposed bedforms (Fig. 9). Particularly
462 prominent changes in dune morphology included the development of trains of superimposed
463 bedforms (Fig. 9, Label S) and flattening of the dune profiles (Fig. 9, Label F). The development of
464 persistent trains of superimposed bedforms was systematically associated with increased water
465 depths and decreased flow velocities (Fig. 10A, Table 2), but was also linked to specific histories of
466 local dune interactions. Trains of superimposed bedforms were found to develop after a dune was
467 overtaken and dissipated into a trough (Fig. 9d,h,m,n,p,r, label S; Table 2). Such dissipation of a dune
468 created an extra-long crest-to-crest distance within which the superimposed bedforms developed
469 (Fig. 9). The association between trains of superimposed dunes and prior loss of an upstream dune
470 was not necessarily found in the inverse situation: not all loss of dunes results in bedform
471 superimposition.

472
473 Flattening of bedforms was more common following a decrease in water depth and an increase in
474 flow velocity (Fig. 10B). No relation was observed between prior dune interactions and flattening of
475 the dune profile. One case was found in which superimposition and flattening of the crest occurred
476 at the same time on successive dunes (Fig. 9d).

477
478 In addition to systematic trains of superimposed bedforms on the stoss slope of a larger dune,
479 superimposed bedforms were also found as solitary and short-lived forms throughout all
480 experiments (Figs 9, 11). Furthermore, small bedforms were common in cases where dunes could
481 not be traced between successive profiles. Such cases led to significant spatial aliasing in our dataset
482 and were labelled as 'instability' of the dune field because the dunes were unable to establish a form
483 of sufficient size and stability to be traced between profiles (e.g. Fig. 9, label U). Instability did not
484 show a clear relation with the changes in flow conditions (Fig. 10C), but was associated with the
485 lower post-change water depths and velocities (Fig. 10D).

486
487 *Interpretation*

488 The results indicate that systematically enhanced superimposition of bedforms (Fig. 1F) is
489 characteristic for the adaptation of the dunes to increased depth and decreased flow velocity,
490 whereas flattening of the dune profile (Fig. 1H) is characteristic for decreased depth and increased
491 flow velocity. The association of spatial aliasing between profiles, the definition of instability within
492 the dune pattern, with post-change flow conditions being considered rather than the magnitude of
493 change, may indicate that dunes potentially become unstable closer to the ripple-to-dune transition
494 (Van den Berg and Van Gelder, 1993) and that smaller bedforms migrate faster in comparison to
495 larger dunes for any given bedload transport rate. The observation that flattening and enhanced
496 bedform superimposition can occur on successive dunes (Fig. 9d) supports the notion that local flow
497 conditions dominate the precise mechanisms of local adaptation of dunes, thus allowing for
498 significant variability in dune shape and process at any stage (Bridge, 1981).

499
500 The observation that trains of superimposed bedforms are associated with increased water depth
501 and decreased flow velocity (clustering in Fig. 10A-B), and locally increased crest-to-crest distances
502 (Fig. 9 label S) is consistent with the experiments of Reesink *et al.* (2014b) and model of Warmink *et al.*
503 (2013), as well as observations of bedform superimposition in rivers during falling stages of floods
504 (Wilbers and Ten Brinke, 2003; Kleinhans *et al.*, 2007). The observation that superimposed bedforms
505 (Fig. 10A) become 'washed-out' (Fig. 10B) following a decrease in water depth is supported by many
506 studies of dune dynamics (Bridge, 1981; Saunderson and Lockett, 1983; Carling *et al.*, 2000; Reesink
507 and Bridge, 2009). However, the association of superimposition and flattening with increases and
508 decreases in flow depth, respectively, presents an apparent contradiction: a decrease in water depth
509 incites dune splitting in a trend towards a larger number of smaller dunes, but, dune splitting

510 requires the development of a superimposed bedform, which is reduced following a decrease in
511 water depth. This apparent contradiction – that the conditions that favour superimposition do not
512 favour dune splitting by superimposed dunes, and vice versa – matches observations of pervasive
513 superimposition on seemingly stable bedforms in natural rivers (Allen 1978; Rubin and McCulloch,
514 1980; Wilbers and Ten Brinke, 2003; Parsons *et al.*, 2005) and suggests that dunes with abundant
515 superimposed bedforms do not necessarily split into smaller dunes.

516
517 This contrast between conditions that favour dune splitting and those that favour the development
518 of superimposed bedforms justifies the recognition of separate classes, and perhaps causes, of
519 superimposition: i) solitary superimposed bedforms that are present throughout the experiments
520 (Mantz, 1978; Bridge, 1981, 2003; Reesink and Bridge, 2009); ii) persistent trains of superimposed
521 bedforms on stable host dunes (Fig. 9, Label S) and iii) the proliferation of small forms in cases where
522 the host dunes are unable to establish a stable morphology. Although these three morphological
523 classes may represent a continuum, their distinction was straightforward for the experimental
524 results herein. Whereas the presence of trains of superimposed bedforms was associated with both
525 overall and local flow conditions, the presence of occasional solitary superimposed bedforms on
526 dunes (cf. Reesink and Bridge, 2009) and thin incipient forms (cf. Venditti *et al.*, 2005) may be
527 independent of flow conditions. These results indicate that the development of solitary
528 superimposed bedforms, rather than the local development of systematic trains of superimposed
529 bedforms, is responsible for dunes splitting.

530 531 **Dune kinematics: addition and loss of dunes from the profiles**

532 Tracing the crests and troughs of dunes between successive bed profiles makes it possible to discern
533 the locations where dunes appear or disappear (Fig. 11, labels + and -). The vertical and horizontal
534 spacing between the crests and troughs varied between profiles in response to changes in dune
535 scour depth and the arrival of superimposed bedforms that modified the shapes of the dune crests
536 and lee slopes. Individual bedform crests were indicated where bedforms could not be traced
537 between successive profiles (Fig. 11, indicated by small circles). A count of the number of dunes lost
538 from, or added to, the profiles provided a measure of dune kinematics (Table 2). The entry and exit
539 of dunes from the test section were not included in this analysis. In the experiments, a total of 26
540 new dunes appeared within the dune profile after the imposed changes in flow as a consequence of
541 splitting and the amalgamation of incipient bedforms that were not classified as dunes (Fig. 11, label
542 +, Table 2). The gain of 26 dunes decreased in the downstream direction with 11, 7, 5, 2 and 1 dunes
543 gained over the 5 metres of the test section. Moreover, 21 dunes were gained in shallower post-
544 change depths (0.17-0.185 m) whereas only 5 dunes were gained in deeper post-change depths
545 (0.19-0.23 m; Table 2). This association of the addition of small dunes in shallower flows was
546 reflected by the clustering of gains of >2 dunes shown in Figure 12B. After the imposed changes in
547 flow, 65 dunes were lost from the test section due to overtaking and merger / amalgamation of
548 dunes, and the dissipation of dunes until the form was no longer traceable (Fig. 11, label -; Table 2).
549 The dissipation of dunes in troughs was often associated with increased scour of the larger new
550 trough (Fig. 9.). The loss of dunes from the profile did not show a clear relationship with
551 downstream distance, post-change conditions, or the magnitude of change (Fig. 12A).

552 553 *Interpretation*

554 The addition and loss of dunes from the profiles provides clear evidence of dune adaptation because
555 the lengthening and shortening of dunes requires dunes to either merge or split. Three key
556 observations can be made. First, more (small) dunes were added to the profile following a decrease
557 in water depth (Fig. 12B), reflecting the destruction of larger dunes in a trend towards smaller dunes
558 that are in equilibrium with the reduced water depth (Ashley, 1990).

559

560 Second, the gain in new (small) dunes was much less than the loss of small dunes to the construction
561 of larger dunes. The splitting of large dunes into a larger number of smaller dunes also decreased in
562 the downstream direction. This dominance of dune construction processes indicates that dunes
563 continued to increase in wavelength throughout the test section. Dunes are known to first approach
564 a stable height, and then continue to amalgamate and interact in a trend towards increasingly stable
565 dune geometries (cf. Gabel *et al.*, 1993; Leclair, 2002; Nabi *et al.*, 2015). The count of gain and loss of
566 the number of dunes indicates that dune stabilization continues throughout the test section, even
567 after dune heights have converged. The analysis of dune loss versus gain provides a more sensitive
568 measure of this continued stabilization than can be achieved through quantification of dune height
569 or wavelength.

570

571 Third, whereas the gain of dunes displayed a downstream trend, the loss of dunes did not. This
572 contrast indicates that the processes of growth and decay are not linearly related, which supports
573 the contention that processes of bedform gain and loss differ fundamentally (cf. Martin and
574 Jerolmack, 2013). The dominance of construction (loss of dunes) over destruction (gain of smaller
575 dunes) also supports the idea that, once established, self-organising flow-form feedbacks stabilise
576 the dunes and allow them to persist: amalgamating smaller bedforms generate new larger bedforms
577 faster, and more easily, than large bedforms split (cf. Fredsøe, 1974; Allen and Friend, 1976; McLean,
578 1990; Bridge, 2003). The observed unevenness in the ease of bedform construction versus the
579 delayed destruction of dunes is, in itself, a contributing factor to dune hysteresis.

580

581 **Analysis of bed elevation distributions**

582 Bed elevation distributions were determined for all profiles in order to provide an analysis of bed
583 topography that was independent from the identification of dunes and their distinction from ripples,
584 transitional bedforms, and ephemeral, incipient, and decayed dunes. When plotted over time, bed
585 elevation distributions visualise the overall developments in dune geometry (Fig. 13). Asymmetrical
586 patterns in the bed elevation distribution over time, in which crest elevation and trough scour
587 develop at different times, were more common than symmetrical increases in bed amplitude where
588 elevation changes occurred at the same time (Fig. 13). Such symmetrical patterns were observed
589 when dunes developed from a low-amplitude bed elevation distribution or a near-flat bed.
590 Superelevation of the dune crest above the average bed elevation distribution only lasted for 5-15
591 minutes and showed no relationship with changes in flow depth or velocity, although a weak
592 association may exist with deeper post-change flow depths (Table 2; 5 of 8 occurrences in the
593 deeper flows and 2 of 15 occurrences in shallow flows). No relationship was found between crest
594 superelevation and flow velocity or Froude number that is linked to the drawdown of the water
595 surface over the crests (Table 2). Contrary to the short-lived superelevation of the dune crests,
596 increased trough scour typically persisted for 15-45 minutes and was associated preferentially with
597 the highest post-change flow velocities (Fig. 13).

598

599 *Interpretation*

600 The analysis of the elevation distribution reveals that dune crests and troughs do not respond to
601 changes in flow at the same time, they do not persist for the same length of time, and they do not
602 respond in the same way to changes in depth and velocity. Whereas trough scour responded more
603 to velocity, superelevation of the dune crest did not, and showed only a weak association with flow
604 depth (Fig. 14). This contrast in the behaviour of crests and troughs matches basic considerations of
605 flow acceleration and deceleration over the dunes. A small change in dune-crest elevation has a
606 proportionally larger effect on flow acceleration over the crest in comparison to the effect of an
607 increase in water depth over the trough. This effect explains the short-lived nature of superelevation
608 of the crest and its preferential association with greater water depths, as opposed to flow velocity.
609 The association of trough scour with greater downstream velocities matches the contention that
610 increased velocity increases turbulence generated by the leeside flow separation shear layer, which

611 increases the potential for scour (Bennett and Best, 1995, 1996; Leclair, 2002; Reesink and Bridge,
612 2009).

613

614 The asymmetrical development of dune trough scour and crest super-elevation matches previous
615 field and flume studies of dune kinematics (Gabel, 1993; Leclair, 2002). The different responses of
616 crests and troughs are in conflict with the general rule that the largest dunes are responsible for the
617 deepest scours and hence the formation and preservation of dune sets (Paola and Borgman, 1991;
618 Leclair and Bridge, 2001). Instead, the relation of trough scour noted herein was often associated
619 with prior dune dissipation (Fig. 9, label S), which suggests that deep scours may be related to
620 interactions of dunes that locally enhance trough scour. Because dune interaction is more
621 pronounced at select times during floods (cf. Martin and Jerolmack, 2013) and at certain locations in
622 natural channels and flumes, the sedimentary record may reflect a more complex set of dune
623 dynamics than merely dune size.

624

625

626 **Analysis of dune deformation (cross-correlation analysis)**

627 The residuals of the cross-correlation of successive profiles (Fig. 7A-B) were plotted in sequence (Fig.
628 7C) to visualise the temporal development of dune deformation in the experiment. This analysis
629 successfully visualises zones of excess, or lack of, deposition relative to the downstream shift of the
630 dune field (Fig. 15). The first observation is that dune deformation is significant, and both spatially
631 and temporally variable. No significant increase in deformation in response to the imposed flow
632 changes, or decrease over time, that would indicate a distinct re-equilibration is observed. Thus,
633 continuous deformation of the dunes as they migrate through the flume dominated over a potential
634 response in dune deformation related to the imposed changes.

635

636 The deformation pattern does not coincide neatly with the dune morphology, as may be expected
637 because the technique separates local deformation of dune geometry from the average dune
638 migration. The differences between dune shape and the magnitude of deformation indicate that the
639 dunes in the experiments of this study change significantly in shape between successive profiles.
640 Despite the complexity of the dune deformation pattern, the gain and loss of sediment is not
641 random, and several, co-existing, deformation patterns can be discerned: 1) consistent zones of
642 gain/loss of sediment that have downstream lengths comparable to the dune wavelength and that
643 persist for 30-60 minutes (black dashed outlines in Fig. 7C and Fig. 15); 2) pronounced gain/loss of
644 sediment from lee slopes over periods that may vary significantly in duration (red and blue lines in
645 Fig. 7C and Fig. 15), and; 3) short-lived and short-wavelength zones of sediment gain/loss that are
646 often not consistent between successive profiles. These three patterns are discussed below.

647

648 The first pattern, zones within which gain or loss dominates over downstream lengths >0.5 m and in
649 periods of time around 30-60 minutes, indicate persistent local sources (red) or sinks (blue) within
650 the dune field (black dashed outlines in Figs 15). Systematic zones of sediment loss and deposition
651 that span across a full dune were observed in cases where dunes dissipated (strict sense cf. Fig. 7D;
652 Fig. 15, Label C) and where dunes grow considerably (strict sense cf. Fig. 7 D; Fig. 15, Label G).
653 Furthermore, large zones of upstream loss and later downstream gain of sediment within the dune
654 profile were associated with the development of superimposed bedforms. These occurrences
655 commonly started when sediment was released locally during the decay of a dune in a trough (Fig.
656 15, label C, dominant red colour). The stoss slope that is located downstream from this decaying
657 dune increases in length (crest-to-crest distance) as a result of the prior dune decay. The lengthened
658 stoss slope is observed to slow down relative to the overall dune migration, which is indicated by its
659 net gain of sediment (Fig. 15, dominant blue colour). The upstream edge of the zone of sediment
660 gain moves downstream in accordance with the decelerated trough. The zone of sediment gain
661 rapidly widens, and then decreases in magnitude over time (Fig. 15, dashed black outlines

662 surrounding blue colour). The onset of a relative gain of sediment on the downstream lee slope is
663 followed by development of superimposed bedforms within the zone of sediment gain (Fig. 6A and
664 Fig. 15h, label S). The temporal development of these zones of sediment gain varies (Fig. 15, Label S,
665 dashed black outlines) and may contain internal variability in deformation related to the
666 development of smaller superimposed bedforms (e.g. Fig. 15h and m). This sequence of associated
667 processes involves successive dunes rather than being limited to a single dune.

668
669 Zones of sediment loss or gain that span an entire dune indicate the decay or growth of this dune
670 (strict sense cf. Fig. 7D). Dune decay (Fig. 15, label C; Table 2) was more common than growth (Fig.
671 15, label G; Table 2), which matches earlier observations of the dominance of the loss of dunes over
672 the gain of dunes. Dune decay was found for most flow conditions (Table 2) and could therefore not
673 be associated with a preferential subset of flow conditions. Dune growth was preferentially
674 associated with increased flow velocities, but because only five clear cases were observed for three
675 flow conditions (Table 2), and other runs with similar flow conditions did not yield comparable
676 results.

677
678 The second apparent pattern is the loss or gain of sediment from lee slopes (Fig. 15, blue and red
679 lines), although not all lee slopes displayed this pattern. Areas of gain or loss of sediment often
680 extended from the lee slope onto the crest or into the trough. The trend in sediment gain or loss
681 could also change half-way down the lee slopes in cases where the shapes of the adjacent crests and
682 troughs changed significantly. Variation in the magnitude of the gain or loss of sediment from the lee
683 slope was commonly linked to the arrival of superimposed bedforms. The arrival of superimposed
684 bedforms, however, did not necessarily change the character of the lee slope from gain to loss of
685 sediment, or vice versa. In other words, superimposed bedforms were seen to affect, but not
686 dominate, the deposition of sediment on the host lee slope. Sediment gain on lee slopes can indicate
687 growth or acceleration of a dune, and sediment loss from lee slopes can indicate its decay or
688 deceleration (Fig. 7D).

689
690 The gain or loss of sediment from the lee slopes persisted for longer (5-60 minutes; Fig. 13; blue and
691 red lines) than clear cases of dune acceleration and deceleration (strict sense cf. Fig. 7D), which
692 require the concurrent movement of both stoss and lee slopes (5-20 minutes; Fig. 15, labels A and
693 D). Acceleration and deceleration of dunes and local growth and decay were common throughout
694 the experiments (Table 2). These dynamics could follow one another temporally on a single dune
695 (Fig. 15 e,k,l,m), and could occur at the same time on successive dunes (Fig. 13 h,k,l,u). Acceleration
696 was common for all changes in flow conditions, and deceleration showed only a slight preference for
697 deeper flows and lower flow velocities (Table 2).

698
699 The third pattern, short-wavelength, short-lived zones of gain or loss of sediment were commonly
700 linked to the presence of superimposed bedforms. However, not all short-lived zones of gain or loss
701 of sediment on dune lee slopes were associated with superimposed bedforms that were easily
702 recognised by the presence of a superimposed stoss and lee slope. Thus, the method also visualises
703 superimposed bedforms on dunes that were incorporated within the dune profile rather than
704 distinguishable based on their own morphology. No clear cases were found in which systematic
705 zones of net gain of sediment (Fig. 15, red colour) were transferred across successive dunes, which
706 would be the expected deformation signature for the through-passing of bedforms (Venditti et al.,
707 2005b). However, it is possible that the temporal resolution of successive profiles in these
708 experiments was not sufficient to reliably resolve this process.

709
710 *Interpretation of dune deformation*
711 The above analysis shows that colouring successive profiles according to the residuals of cross-
712 correlation visualises successfully the local gain or loss of sediment within the mobile dune field (Figs

713 7, 15). No appreciable change in the magnitude of deformation was found in relation to the imposed
714 changes in flow, indicating that adaptation did not significantly enhance deformation relative to the
715 migration of the bedforms. Additionally, it is likely that deformation associated with the downstream
716 development of dunes as they migrated through the flume dominated any increase of deformation
717 induced by imposed changes in flow depth and velocity. The previous sections indicate, however,
718 that individual processes did change systematically in both magnitude and frequency. The
719 deformation pattern that is revealed illustrates that the deformation of dunes is significant and
720 highly variable across the dune profiles, as well as over time. To guide the interpretation of this new
721 visualisation of dune deformation, three patterns are highlighted.

722

723 The first pattern, zones of relative gain or loss of sediment that persist systematically within the
724 mobile dune field, can be interpreted as local sources and sinks of sediment: they attract or shed
725 sediment as the dunes migrate downstream. Zones of systematic gain of sediment on stoss slopes
726 appear to be associated with the development of trains of superimposed bedforms. It is important
727 to emphasise that such a 'gain' is relative to the motion of the dune field, and presents a decrease in
728 erosion of the stoss slope rather than net deposition or upstream migration. The development of
729 trains of bedforms within zones of sediment gain highlight that: i) defects within a dune field are
730 dissipated over time as sediment is dispersed across dunes, and ii) the dissipation of defects within a
731 dune field occurs through a series of associated processes rather than a single mechanism.

732

733 The second pattern, sediment loss and gain on lee slopes, is pronounced because the largest volume
734 of deposition occurs on the lee slope, and this creates the largest potential for relative changes in
735 deposition. The variability in relative deposition on lee slopes emphasises the importance of
736 differential migration (Fig. 1 D; cf. Martin and Jerolmack, 2013), although the lee slope alone is not
737 evidence for acceleration or deceleration of dunes (cf. Fig. 7D). Dune acceleration and deceleration
738 were predominantly short-lived, which reflects that dunes are pinned in place by the flow to their
739 upstream and downstream counterparts. The results thus indicate that, rather than 'jostling for
740 position without coalescing' (Coleman and Melville, 1994, p555), significant transfer of sediment
741 occurs between dunes.

742

743 The loss of sediment commonly extends beyond the lee slope onto the adjacent crest and/or trough.
744 Decreased deposition on the lee slope directly downstream from a dune crest that is losing sediment
745 (Fig. 15, red colour) is a signature that is likely associated with bypassing of sediment, and hence
746 transfer of sediment between dunes (Naqshband et al., 2014a). Decreased deposition on a lee slope
747 upstream from a trough that is deepening likely reflects the continuation of sediment transport in
748 the trough while the lee slope receives little sediment, such as is the case when the trough of a
749 superimposed bedform reaches the crest of its host dune (Fernandez et al., 2006; Reesink and
750 Bridge, 2007, 2009).

751

752 This final pattern, short-lived local variations in gain or loss of sediment that are often aliased
753 spatially between successive profiles, was commonly associated with the presence of superimposed
754 bedforms. Thus, the results highlight the importance of bedform superimposition as a control on
755 sediment redistribution over successive dunes. The abundance of short-lived local variability, as well
756 as partial growth, decay, splitting, and merger found in these experiments highlights that the dunes
757 are far less stable than would be inferred from their traditional description as individual entities.
758 Critically, this analysis illustrates that dune deformation is dominated by dune-to-dune interactions
759 that occur on spatial scales of 0.1 to 2 m and temporal scales of several minutes to hours. These
760 scales are too large and long-lasting to be linked to individual coherent flow structures and too small
761 to be the sole product of imposed flow conditions: dune deformation thus reflects a multitude of
762 form-flow feedback processes that operate between the scales of turbulence and those at which
763 average flow parameters are established.

764
765
766
767
768
769
770
771
772
773
774
775
776
777
778
779
780
781
782
783
784
785
786
787
788
789
790
791
792
793
794
795
796
797
798
799
800
801
802
803
804
805
806
807
808
809
810
811
812

DISCUSSION

The adaptation of dunes to changes in flow is the end-product of multiple, simultaneous processes that redistribute sediment over and among dunes (Fig. 1). The same sediment redistribution processes are also responsible for the steady-state deformation of dunes (see McElroy and Mohrig, 2009). The present study illustrates that this sediment redistribution is pervasive, and hence dunes are far more interconnected than has been commonly acknowledged when treating them as individual and measurable entities.

Although the present experiments with mobile dunes in shallow flows (depth 0.17-0.25 m) indicate that many of the individual processes involved in the deformation of dunes respond in their own unique way to changes in flow velocity and depth. Although these findings are in line with those of detailed flow quantifications by Unsworth *et al.* (in press), the development of quantification or predictive models would be premature based on the present dataset. The fully-mobile sand-bed experiments presented herein include significant spatial and temporal variability in flow, bed morphology, and adaptation processes, and the data represent two-dimensional slices through dunes that possess a three-dimensional character. Nonetheless, the new tools for analysis and visualisation of changes in dune morphology presented herein provide the basis for a series of unique observations with important implications for the way we consider the spatial variability in dune geometry, dune development and hysteresis, the form-flow equilibrium of subaqueous dunes, and sediment transport over dunes.

Dune morphology responds differently to changes in flow depth and velocity

The results of the present experimental study of dunes in shallow flows (depth 0.17-0.25 m) confirm that the adaptation of dunes, and the manner in which sediment is redistributed across the form, is not a simple function of sediment transport rates (Allen 1982). Instead, different geometric signatures were observed for dunes adapting to changes in water depth and flow velocity. Six main findings are apparent:

- i) In the experiments, the magnitude of dune deformation (Figs 7, 15) did not change systematically directly following the imposed change in flow. The absence of a clear change in the magnitude of deformation is partially attributed to the limited ranges of flow depth and velocity in the experiments. Instead of a significant change in the magnitude of deformation, adaptation occurred through systematic changes in the processes that controlled the redistribution of sediment over and across dunes (Fig. 1).
- ii) Trough scour (Fig. 14A) increased following an increase in velocity, and was linked to local dune interactions and bedform overtaking.
- iii) Flattening of the dune crest (Fig. 10B) increased following an increase in flow velocity and/or a decrease in water depth.
- iv) The development of trains of superimposed bedforms was associated with an increase in flow depth and a decrease in flow velocity (Fig. 10A) and was linked to prior decay of an upstream dune. This dune decay created an increased crest-to-crest distance, and led to the deceleration (relative to the surrounding dunes) of the stoss slope on which the superimposed bedforms developed.
- v) Acceleration and deceleration, and growth and decay of dunes, were common in most experimental runs and showed no clear association with changes in flow depth or velocity (Table 2), although their magnitudes may vary depending on flow conditions (Martin and Jerolmack, 2013).

813 vi) Instability of the dune pattern, indicated by spatial aliasing between successive profiles,
814 was more common in shallow flows (Fig. 10D) and was unaffected by the direction or
815 magnitude of change (Fig. 10C).

816 Thus, dune adaptation processes differ for changes in flow depth and velocity, and may be
817 dominated by: 1) the imposed change in the flow conditions, 2) the post-change flow conditions, and
818 3) local form-flow feedback processes.

819

820 **Temporal variability in dune adaptation: types of hysteresis**

821 The present study highlights that the complex nature of dune development is subject to at least
822 three different types of hysteresis: 1) *apparent hysteresis* created by a temporal lag in response of
823 dunes to the flow, 2) *true hysteresis* in which growth and decay are caused by fundamentally
824 different processes, and 3) a *hysteresis of the driving variables* created by the out-of-phase relation
825 between water depth and velocity during the passage of flood waves (Figs 2, 3, 16).

826

827 The best known form of hysteresis is the temporal development lag or '*apparent hysteresis*', in
828 which the redistribution of sediment over and among dunes takes time, such that bedform
829 adaptation lags behind relative to the change in flow (Allen, 1973, 1974, 1982; Julien and Klaassen,
830 1995; Wilbers *et al.*, 2003; Shimizu *et al.*, 2009). In addition, the present study and recent work by
831 Martin and Jerolmack (2013) suggests that the processes of dune growth and decay differ
832 fundamentally. The results presented herein support the notion that dunes prolong their existence
833 through the development of a persistent separated flow in their lee, which is, by itself, a cause of
834 hysteresis (Fredsoe, 1974; Allen and Friend, 1976; McLean, 1990). When the loop-like relation
835 between dune form and flow is a consequence of fundamentally different processes, this is known
836 as '*true hysteresis*'. The distinction between true and apparent hysteresis is particularly important
837 because apparent hysteresis can be modelled as a function of sediment transport and would reflect
838 dunes in all environments (Allen, 1973, 1974), whereas true hysteresis requires a more complex
839 treatment of different growth and decay mechanisms. The present study emphasises the
840 importance of simultaneous processes of sediment re-distribution (Fig. 1), which have a specific
841 preference for rising or falling flow stages because they relate differently to flow depth and velocity.
842 Finally, water depth and the water-surface slope that drives the flow velocity are out-of-phase
843 during the passage of flood waves (Fig. 14). This out-of-phase relation between water depth and
844 water-surface slope during flood waves can be seen as a '*hysteresis of the driving variables*' (Figs 2,
845 3).

846

847 The systematic, out-of-phase changes in water depth and flow velocity during the passage of flood
848 waves will result in systematically altered behaviour of the dunes, which is summarised as a
849 conceptual diagram (Fig. 16). Morphological responses, such as flattening of the dune crest (e.g.
850 Carling *et al.*, 2000), increased trough scour (e.g. Gabel, 1993), and the development of trains of
851 superimposed bedforms, were associated with specific depth-velocity combinations, and should
852 therefore vary in a similar fashion during the passage of a flood wave in a straight, shallow channel.
853 The passage of successive flood waves will result in cyclic repetition of these processes of dune
854 growth and decay, which is expected to be predictable for individual locations, but not necessarily
855 transferable between locations because of spatial variability in the controls on dune adaptation.

856

857 **Spatial and environmental variability in dune adaptation**

858 The hydraulic controls on dune adaptation vary spatially within and between depositional
859 environments. In river channels, water depth and water surface slope vary spatially between the
860 thalweg and bar tops, across bends, along the catchment from the headwaters, through lowland
861 rivers and the backwater zone to tidally-influenced reaches (Fig. 4; Leopold and Maddock, 1953;
862 Knighton, 1999). Locally, flow depth and velocity vary dramatically in their relative magnitude from

863 the thalweg to bar tops (Fig. 4). This may be most apparent when considering the abandonment of
864 dunes on bar-tops, in oxbow lakes, and in bar troughs (Reesink et al., 2015). It may be expected that
865 the processes shown in Figure 16 need to be reviewed critically when this conceptual model of cyclic
866 dune development is applied to different areas within river channels. The controlling parameters
867 also vary systematically along rivers. In particular, the main channels of the world's largest rivers are
868 characterised by deep flows and low water-surface slopes. This combination of hydraulic parameters
869 that control dune development provides an explanation for differences in the behaviour of dunes in
870 such large rivers in comparison to those seen in smaller channels and flume experiments (Julien and
871 Klaassen, 1995; Amsler and Garcia, 1997).

872

873 The shapes of flood waves also vary between rivers. The large annual floods in monsoon-cyclone
874 systems such as the Mekong River (Darby et al., 2016) are likely to contrast with more asymmetrical
875 flood waves in the Mississippi River that respond to snow melt, rainfall, and groundwater recharge
876 (Fig. 3). Whereas the absolute magnitude of the floods determines the absolute and relative changes
877 in depth and velocity, the asymmetry of the flood wave determines the relative duration of various
878 stages of the out-of-phase cycle of depth and water surface slope (Fig. 16). For example, the
879 common observation of cannibalization of host dunes by smaller superimposed dunes (e.g. Pretious
880 and Blench, 1951; Julien and Klaassen, 1995; Wilbers et al., 2003; Kleinhans et al., 2007) may
881 become more pronounced with longer duration waning stages of floods.

882

883 The results of the present study show that dune adaptation varies in response to different
884 controlling parameters (e.g. depth, velocity, viscosity, magnitudes of change, gravitational
885 acceleration). The hydraulic controls are even more variable when non-fluvial environments, such as
886 estuaries, shallow-marine zones, submarine density currents, and aeolian deserts are considered.
887 Thus, the summary of the experimental results depicted in Fig. 16 does not necessarily describe
888 dunes in deep flows, or dunes in tidal and tidally-influenced channels, where frequent flow reversals
889 and changes in velocity affect the dynamic development of dunes. Although the similarity in the
890 form of asymmetrical sandy bedforms in different environments suggests that overarching principles
891 can be identified, the results shown herein suggest that the processes that control dune adaptation
892 need to be compared and contrasted between different locations and environments.

893

894 **Equilibration of dunes: from local interactions to long-distance transfer**

895 Dune height is known to develop faster than dune wavelength (cf. Gabel, 1993; Leclair, 2002), and
896 this contention is further supported by the present results. After mean dune height and wavelength
897 achieve stable values, the equilibration of dunes continues by means of kinematic interactions,
898 which continued throughout the entire length of the present mobile bed experiments. Some
899 deformation processes were found to generate others. For example, dissipation of a dune was
900 commonly followed by the appearance of superimposed bedforms on the downstream dune stoss
901 slope. The transfer of sediment through chains of associated processes introduces an important
902 problem: the trend towards equilibrium dune geometries requires merging and splitting of dunes
903 (Fig. 1 A,B), which generates local instabilities within the dune field that then need to be dissipated.
904 Indeed, even after stable dune heights and wavelengths have been attained, "jostling for position
905 without coalescing" is known to continue (Coleman and Melville, 1994, p.555). The visualisation and
906 analysis of dune deformation illustrated herein illustrates that this jostling is a proliferation of
907 interactions between dunes, rather than spatial re-adjustment of dunes that maintain their size and
908 shape. The size and abundance of sources and sinks of sediment within the dune field will likely
909 decrease as dunes approach their equilibrium geometry, and a change will necessarily take place
910 from local interactions to longer-distance transfer of excess sediment over increasingly stable dunes.
911 Thus, the present study provides a framework for the interpretation of quantitative data from
912 bedload sampling (e.g. Emmett, 1979) and acoustic measurements of bedload velocity and
913 concentration (Rennie et al., 2002; Kostaschuk et al., 2009; Naqshband et al., 2014a). Sediment

914 transport over dune-covered river beds is perhaps better described as the sum of changing, local,
915 form-flow interactions, rather than a steady flux that is set by reach-averaged flow conditions.

916

917 **New methods for investigating the dynamic development of dunes**

918 Whereas the quantification of characteristic dune heights and wavelengths (Van der Mark et al.,
919 2008) provides a sound basis for estimates of mean bed roughness, the reduction of complex dune
920 patterns into simple descriptors hinders detailed analyses of the many form-flow feedback processes
921 that control dune development. In order to avoid oversimplification of the initial evidence, four
922 complementary methods that highlight different aspects of dune development are presented herein,
923 each with its own merit and drawbacks. The visual classification of aspects of dune morphology (Figs
924 6, 9) is easy, but may be sensitive to subjective interpretation. The quantification of dune kinematics
925 through counting of the gain and loss of dunes (Figs 6, 11) is easy and objective, but also combines
926 different morphodynamic processes (see Gabel, 1993; Warmink et al., 2014) that may well respond
927 differently to changes in flow and the evolution of the surrounding bed morphology. The use of a
928 bed-elevation distribution (Figs 6, 13) is an objective way to assess dune morphology, but is sensitive
929 to the size of the area of measurement, superimposition of bedforms and the presence of larger-
930 scale bed forms. The visualisation of bed deformation by plotting the residuals of a cross-correlation
931 between successive dune profiles (Figs 7, 15) has been shown to be a practical method for
932 generating objective evidence of the dynamic development of dunes. However, determining its full
933 value and limitations will require further application to data from a wide range of contrasting
934 environments such as rivers, estuaries, oceans and deserts.

935

936

937

CONCLUSIONS

938

939 The present study illustrates how dunes adapt to changes in a unidirectional flow. Dunes compete
940 for space as they grow or decay in response to changing flow depth and velocity, and this creates
941 local sources and sinks of sediment within the mobile dune field. These local instabilities induce
942 significant sediment redistribution over, and between, dunes, which occurs through multiple,
943 simultaneously acting processes. Dune adaptation is a spatially- and temporally- variable response of
944 multiple, interacting dunes.

945

946 The present illustrate that dunes respond differently to changes in flow depth and velocity in the
947 present shallow experimental flows. The most prominent morphological responses include: i) an
948 increase in bedform superimposition following an increase in depth and velocity, ii) the flattening of
949 dunes in response to decreased flow depth, and iii) an increase in scour in response to increased
950 flow velocity. Variation in the response of dunes to changes in flow depth and velocity is particularly
951 important, because the magnitude of flow depth and velocity vary systematically over time during
952 floods, and spatially across and along river channels.

953

954 The analyses developed herein provide a new, objective, basis for the analysis of the processes that
955 control the dynamic development of bedforms in the temporally and spatially complex flows of
956 different environments on Earth as well as other planetary bodies.

957

958

959 **ACKNOWLEDGMENTS**

960

961 This research was supported by grant NE/I014101/1 from the UK Natural Environment Research
962 Council (NERC). Data can be accessed by contacting A. Reesink. The manuscript has been improved
963 significantly based on the thorough and constructive reviews of prof. Stéphane Rodrigues and prof.
964 Burghard Flemming, for which we are very grateful.

965

966 **REFERENCES**

967

968 Allen, J. R. L., 1973. Phase differences between bed configuration and flow in natural environments,
969 and their geological relevance. *Sedimentology*, 20(2), 323-329, doi:10.1111/j.1365-
970 3091.1973.tb02054.x.

971 Allen, J. R. L., 1974. Reaction, relaxation and lag in natural sedimentary systems: General principles,
972 examples and lessons. *Earth Sci. Rev.*, 10(4), 263-342. [https://doi.org/10.1016/0012-
973 8252\(74\)90109-3](https://doi.org/10.1016/0012-8252(74)90109-3)

974 Allen, J. R. L., 1978. Polymodal dune assemblages: An interpretation in terms of dune creation-
975 destruction in periodic flows. *Sediment. Geol.*, 20, 17-28. [https://doi.org/10.1016/0037-
976 0738\(78\)90046-5](https://doi.org/10.1016/0037-0738(78)90046-5)

977 Allen, J. R. L., Friend, P. F., 1976. Relaxation time of dunes in decelerating aqueous flows. *J. Geol. Soc.*
978 London, 132(1), 17-26. <https://doi.org/10.1144/gsjgs.132.1.0017>

979 Allen, J. R. L., Collinson, J. D. 1974. The superimposition and classification of dunes formed by
980 unidirectional aqueous flows. *Sedimentary Geology*, 12(3), 169-178.
981 [https://doi.org/10.1016/0037-0738\(74\)90008-6](https://doi.org/10.1016/0037-0738(74)90008-6)

982 Allen, J.R.L., 1982. *Sedimentary Structures, their Character and Physical Basis*, volumes 1- 2.
983 *Developments in Sedimentology 30 a & b*. Elsevier Scientific Publishing Company, Amsterdam.

984 Almeida, R. P., Galeazzi, C. P., Freitas, B. T., Janikian, L., Ianniruberto, M., Marconato, A., 2016. Large
985 barchanoid dunes in the Amazon River and the rock record: Implications for interpreting large
986 river systems. *Earth and Planetary Science Letters*, 454, 92-102.
987 <https://doi.org/10.1016/j.epsl.2016.08.029>

988 Amsler, M.L. and Garcia, M.H., 1997. Sand-dune geometry of large rivers during floods – Discussion.
989 *J. Hydraul. Eng.*, 123, 582–585.

990 Ashley, G. M., 1990. Classification of large-scale subaqueous bedforms: a new look at an old

991 Baas, J. H., and Best, J. L., 2002. Turbulence modulation in clay-rich sediment-laden flows and some
992 implications for sediment deposition. *Journal of Sedimentary Research*, 72(3), 336-340.
993 doi: 10.1306/120601720336

994 Baas, J. H., Best, J. L., Peakall, J., & Wang, M., 2009. A phase diagram for turbulent, transitional, and
995 laminar clay suspension flows. *Journal of Sedimentary Research*, 79(4), 162-183.

996 Baas, J.H., Best, J.L. and Peakall, J. 2016. Predicting bedforms and primary current lamination in
997 cohesive mixtures of mud and sand, *J. Geological Society of London.*, 173, 12-45, doi:
998 10.1144/jgs2015-024.

999 Bennett, S. J., and Best, J. L., 1995. Mean flow and turbulence structure over fixed, two-dimensional
1000 dunes: Implications for sediment transport and bedform stability. *Sedimentology*, 42(3), 491-
1001 513. DOI:10.1111/j.1365-3091.1995.tb00386.x

1002 Bennett, S.J. & Best, J.L. 1996. Mean flow and turbulence structure over fixed ripples and the ripple-
1003 dune transition. In: *Coherent flow structures in open channels*, (Eds: Ashworth, P.J., Bennett, S.J.,
1004 Best, J.L. and McLelland, S.J.), Wiley and Sons, 281-304.

1005 Best, J.L. 1993 On the interactions between turbulent flow structure, sediment transport and
1006 bedform development: some considerations from recent experimental research. In: *Turbulence:
1007 perspectives on flow and sediment transport*, (Eds: Clifford, N., French, J.R. and Hardisty, J), 61-
1008 92. Wiley and Sons.

1009 Best, J.L. 1996 The fluid dynamics of small-scale alluvial bedforms. In: *Advances in Fluvial Dynamics
1010 and Stratigraphy* (Eds: Carling, P.A. and Dawson, M.), 67-125, Wiley and Sons.

1011 Best, J., 2005a. The fluid dynamics of river dunes: A review and some future research
1012 directions. *Journal of Geophysical Research: Earth Surface*, 110(F4). DOI:10.1029/2004JF000218

1013 Best, J. L., 2005b. Kinematics, topology and significance of dune-related macroturbulence: some
1014 observations from the laboratory and field. *Fluvial sedimentology VII*, 35, 41-60.

1015 Best, J., and Kostaschuk, R. 2002. An experimental study of turbulent flow over a low-angle
1016 dune. *Journal of Geophysical Research: Oceans*, 107(C9). DOI: 10.1029/2000JC000294

1017 Best, J.L., Ashworth, P.J., Sarker, M.H. and Roden, J.E., 2007. The Brahmaputra-Jamuna River,
1018 Bangladesh. In: Large Rivers; Geomorphology and Management (Ed. A. Gupta), pp. 395–430.
1019 John Wiley & Sons Ltd, Chichester.

1020 Best, J., Simmons, S., Parsons, D., Oberg, K., Czuba, J., Malzone, C., 2010. A new methodology for the
1021 quantitative visualization of coherent flow structures in alluvial channels using multibeam echo-
1022 sounding (MBES). *Geophysical Research Letters*, 37(6). DOI: 10.1029/2009GL041852

1023 Blom, A., Ribberink, J. S., and de Vriend, H. J., 2003. Vertical sorting in bed forms: Flume experiments
1024 with a natural and a trimodal sediment mixture. *Water Resources Research*, 39(2).
1025 DOI: 10.1029/2001WR001088

1026 Blom, A., Parker, G., Ribberink, J. S., and De Vriend, H. J., 2006. Vertical sorting and the
1027 morphodynamics of bed-form-dominated rivers: An equilibrium sorting model. *Journal of*
1028 *Geophysical Research: Earth Surface*, 111(F1). DOI: 10.1029/2004JF000175

1029 Bradley RW, Venditti JG., 2017. Reevaluating dune scaling relations. *Earth-Science Reviews*, 165,
1030 356–376. <https://doi.org/10.1016/j.earscirev.2016.11.004>

1031 Bridge, J. S., 1981. Bed shear stress over subaqueous dunes, and the transition to upper-stage plane
1032 beds. *Sedimentology*, 28(1), 33-36. DOI: 10.1111/j.1365-3091.1981.tb01660.x

1033 Bridge, J. S. 1993. The interaction between channel geometry, water flow, sediment transport and
1034 deposition in braided rivers. *Geological Society, London, Special Publications*, 75(1), 13-71.
1035 <https://doi.org/10.1144/GSL.SP.1993.075.01.02>

1036 Bridge, J.S., 2003. Rivers and Floodplains; Forms, Processes, and Sedimentary Record. Blackwell
1037 Publishing, Oxford, U.K., 600 pp.

1038 Carling, P. A., 1991. An appraisal of the velocity-reversal hypothesis for stable pool-riffle sequences
1039 in the River Severn, England. *Earth Surface Processes and Landforms*, 16(1), 19-31.
1040 DOI: 10.1002/esp.3290160104

1041 Carling PA, Golz E, Orr HG, Radecki-Pawlik A., 2000. The morphodynamics of fluvial sand dunes in the
1042 River Rhine, near Mainz, Germany. I. Sedimentology and morphology. *Sedimentology*, 47(1):227-
1043 52. DOI: 10.1046/j.1365-3091.2000.00290.x

1044 Church, M., Ferguson, R. I., 2015. Morphodynamics: Rivers beyond steady state. *Water Resources*
1045 *Research*, 51(4), 1883-1897. DOI: 10.1002/2014WR016862

1046 Claude, N., Rodrigues, S., Bustillo, V., Bréheret, J.-G., Macaire, J.-J., Jugé, P., 2012. Estimating bedload
1047 transport in a large sand–gravel bed river from direct sampling, dune tracking and empirical
1048 formulas. *Geomorphology* 179, 40–57. <https://doi.org/10.1016/j.geomorph.2012.07.030>

1049 Coleman, S. E., and Melville, B. W., 1996. Initiation of bed forms on a flat sand bed. *Journal of*
1050 *Hydraulic Engineering*, 122(6), 301-310. [https://doi.org/10.1061/\(ASCE\)0733-](https://doi.org/10.1061/(ASCE)0733-9429(1996)122:6(301))
1051 [9429\(1996\)122:6\(301\)](https://doi.org/10.1061/(ASCE)0733-9429(1996)122:6(301))

1052 Coleman, S. E., and Nikora, V. I., 2011. Fluvial dunes: initiation, characterization, flow
1053 structure. *Earth Surface processes and landforms*, 36(1), 39-57. DOI: 10.1002/esp.2096

1054 Coleman, S. E., Nikora, V. I., and Aberle, J., 2011. Interpretation of alluvial beds through bed-
1055 elevation distribution moments. *Water Resources Research*, 47(11).
1056 DOI: 10.1029/2011WR010672

1057 Cutts, J. A., and Smith, R. S. U., 1973. Eolian deposits and dunes on Mars. *Journal of Geophysical*
1058 *Research*, 78(20), 4139-4154. DOI: 10.1029/JB078i020p04139

1059 Dalrymple, R.W., Kurcinka C.E., Jablonski B.V.J., Ichaso A.A., Mackay D.A., 2015. Deciphering the
1060 relative importance of fluvial and tidal processes in the fluvial–marine transition. in Ashworth,
1061 P.J., Best, J.L., and Parsons D.R. (Eds.) *Fluvial Tidal Sedimentology*, Advances in Sedimentology
1062 Vol. 68. Elsevier.

1063 Darby, S. E., Hackney, C. R., Leyland, J., Kummu, M., Lauri, H., Parsons, D. R., Best, J.L., Nicholas, A.P.,
1064 Aalto, R., 2016. Fluvial sediment supply to a mega-delta reduced by shifting tropical-cyclone
1065 activity. *Nature*, 539(7628), 276-279. doi:10.1038/nature19809

1066 Dawdy, D. R., 1965. Discontinuous depth-discharge relations for sand-channel streams and their
1067 effect on sediment transport. In *Proceedings of the Federal Inter-Agency Sedimentation*
1068 *Conference, 1963* (No. 970, p. 309). US Department of Agriculture.

1069 Diniega, S., Krevalevsky, M., Radebaugh, J., Silverstro, S., Telfer, M., Tirsch, D., 2016. Our evolving
1070 understanding of aeolian bedforms, based on observation of dunes on different worlds. *Aeolian*
1071 *Research*. <https://doi.org/10.1016/j.aeolia.2016.10.001>

1072 Ditchfield, R., and Best, J., 1992. Discussion of "Development of Bed Features" by Arved J. Raudkivi
1073 and Hans-H. Witte (September, 1990, Vol. 116, No. 9). *Journal of Hydraulic Engineering*, 118(4),
1074 647-650.

1075 Emmett, W. W. 1979. *A field calibration of the sediment-trapping characteristics of the Helley-Smith*
1076 *bedload sampler* (Vol. 1139). US Government Printing Office.

1077 Ewing, R. C., & Kocurek, G. A. 2010. Aeolian dune interactions and dune-field pattern formation:
1078 White Sands Dune Field, New Mexico. *Sedimentology*, 57(5), 1199-1219. DOI: 10.1111/j.1365-
1079 3091.2009.01143.x

1080 Fernandez, R., Best, J., López, F., 2006. Mean flow, turbulence structure, and bed form
1081 superimposition across the ripple-dune transition. *Water Resources Research*, 42(5).
1082 DOI: 10.1029/2005WR004330

1083 Flemming, B. W., and Bartholomä, A. 2012. Temporal variability, migration rates and preservation
1084 potential of subaqueous dune fields generated in the Agulhas Current on the southeast African
1085 continental shelf. *Sediments, Morphology and Sedimentary Processes on Continental Shelves:*
1086 *Advances in Technologies, Research, and Applications*, 229-247.

1087 Flemming, B. W. 2000. The role of grain size, water depth and flow velocity as scaling factors
1088 controlling the size of subaqueous dunes. In *Marine Sandwave Dynamics, international*
1089 *workshop* (pp. 23-24).

1090 Fredsøe, J. 1974. On the development of dunes in erodible channels. *Journal of Fluid*
1091 *Mechanics*, 64(01), 1-16. DOI: <https://doi.org/10.1017/S0022112074001960>

1092 Frings, R. M., Kleinhans, M. G., 2008. Complex variations in sediment transport at three large river
1093 bifurcations during discharge waves in the river Rhine. *Sedimentology*, 55(5), 1145-1171.
1094 DOI: 10.1111/j.1365-3091.2007.00940.x

1095 Gabel, S. L., 1993. Geometry and kinematics of dunes during steady and unsteady flows in the
1096 Calamus River, Nebraska, USA. *Sedimentology*, 40(2), 237-269. DOI: 10.1111/j.1365-
1097 3091.1993.tb01763.x

1098 García, M.H., 2006. ASCE Manual of Practice 110—Sedimentation Engineering: Processes,
1099 Measurements, Modeling and Practice. [https://doi.org/10.1061/40856\(200\)94](https://doi.org/10.1061/40856(200)94)

1100 Giri, S., Shimizu, Y., 2006. Numerical computation of sand dune migration with free surface
1101 flow. *Water Resources Research*, 42(10). DOI: 10.1029/2005WR004588

1102 Hoey, T. B., Ferguson R., 1994. Numerical simulation of downstream fining by selective transport in
1103 gravel bed rivers: Model development and illustration, *Water Resour. Res.*, 30(7), 2251–2260,
1104 doi:[10.1029/94WR00556](https://doi.org/10.1029/94WR00556).

1105 Jerolmack, D. J., Mohrig, D., 2005. Frozen dynamics of migrating bedforms. *Geology*, 33(1), 57-60.
1106 <https://doi.org/10.1130/G20897.1>

1107 Jackson, R. G., 1975. Velocity–bed-form–texture patterns of meander bends in the lower Wabash
1108 River of Illinois and Indiana. *Geological Society of America Bulletin*, 86(11), 1511-1522.
1109 [https://doi.org/10.1130/0016-7606\(1975\)86<1511:VPOMBI>2.0.CO;2](https://doi.org/10.1130/0016-7606(1975)86<1511:VPOMBI>2.0.CO;2)

1110 Jackson, R. G., 1976. Large scale ripples of the lower Wabash River. *Sedimentology*, 23(5), 593-623.
1111 DOI: 10.1111/j.1365-3091.1976.tb00097.x

1112 Jopling, A. V., 1965. Hydraulic factors controlling the shape of laminae in laboratory deltas. *Journal of*
1113 *Sedimentary Research*, 35(4).

1114 Julien, P. Y., and Klaassen, G. J. 1995. Sand-dune geometry of large rivers during floods. *Journal of*
1115 *Hydraulic Engineering*, 121(9), 657-663. [https://doi.org/10.1061/\(ASCE\)0733-](https://doi.org/10.1061/(ASCE)0733-9429(1995)121:9(657))
1116 [9429\(1995\)121:9\(657\)](https://doi.org/10.1061/(ASCE)0733-9429(1995)121:9(657))

1117 Julien, P. Y., Klaassen, G. J., Ten Brinke, W. B. M., Wilbers, A. W. E., 2002. Case study: bed resistance
1118 of Rhine River during 1998 flood. *Journal of Hydraulic Engineering*, 128(12), 1042-1050.
1119 [https://doi.org/10.1061/\(ASCE\)0733-9429\(2002\)128:12\(1042\)](https://doi.org/10.1061/(ASCE)0733-9429(2002)128:12(1042))

1120 Kleinhans, M. G., 2004. Sorting in grain flows at the lee side of dunes. *Earth-Science Reviews*, 65(1),
1121 75-102. [https://doi.org/10.1016/S0012-8252\(03\)00081-3](https://doi.org/10.1016/S0012-8252(03)00081-3)

1122 Kleinhans, M. G., Wilbers, A. W. E., Ten Brinke, W. B. M., 2007. Opposite hysteresis of sand and
1123 gravel transport upstream and downstream of a bifurcation during a flood in the River Rhine, the
1124 Netherlands. *Netherlands Journal of Geosciences/Geologie en Mijnbouw*, 86(3).

1125 Kleinhans, M. G., Leuven, J. R. F. W., Braat, L., Baar, A. 2017. Scour holes and ripples occur below the
1126 hydraulic smooth to rough transition of movable beds. *Sedimentology*, 64(5), 1381–1401,
1127 doi:10.1111/sed.12358

1128 Knighton, A. D., 1999. Downstream variation in stream power. *Geomorphology*, 29(3), 293-306.
1129 [https://doi.org/10.1016/S0169-555X\(99\)00015-X](https://doi.org/10.1016/S0169-555X(99)00015-X)

1130 Kocurek, G., and Ewing, R. C., 2005. Aeolian dune field self-organization—implications for the
1131 formation of simple versus complex dune-field patterns. *Geomorphology*, 72(1), 94-105.
1132 <https://doi.org/10.1016/j.geomorph.2005.05.005>

1133 Kostaschuk, R., Shugar, D., Best, J., Parsons, D., Lane, S., Hardy, R., Orfeo, O., 2009. Suspended
1134 sediment transport and deposition over a dune: Río Paraná, Argentina. *Earth Surface Processes
1135 and Landforms*, 34(12), 1605-1611. DOI: 10.1002/esp.1847

1136 Kwoil, E., Venditti, J. G., Bradley, R. W., and Winter, C., 2016. Flow structure and resistance over
1137 subaqueous high-and low-angle dunes. *Journal of Geophysical Research: Earth Surface* 121,
1138 545–564 DOI: 10.1002/2015JF003637

1139 Leclair, S. F., Bridge, J. S., 2001. Quantitative interpretation of sedimentary structures formed by
1140 river dunes. *Journal of Sedimentary Research*, 71(5), 713-716.

1141 Leclair, S. F. 2002. Preservation of cross-strata due to the migration of subaqueous dunes: an
1142 experimental investigation. *Sedimentology*, 49(6), 1157-1180 DOI: 10.1046/j.1365-
1143 3091.2002.00482.x

1144 Leeder, M.R., 1983. On the interactions between turbulent flow, sediment transport and bedform
1145 mechanics in channelized flows. In: Collinson, J.D., and Lewin, J., eds., *Modern and ancient fluvial
1146 systems*: IAS Special Publications 6, 5-18. DOI: 10.1002/9781444303773.ch1

1147 Lefebvre, A., Paarlberg, A. J., Winter, C., 2016. Characterising natural bedform morphology and its
1148 influence on flow. *Geo-Marine Letters*, 1-15. DOI 10.1007/s00367-016-0455-5

1149 Leopold, L. B., Maddock, T., 1953. *The hydraulic geometry of stream channels and some
1150 physiographic implications* (Vol. 252). US Government Printing Office.

1151 Malarkey, J., Baas, J.H., Hope, J.A., Aspden, R.J., Parsons, D.R., Peakall, J., Paterson, D.M., Schindler
1152 R.J., Ye L., Lichtman I.D., Bass, S.J., Davies A.G, Manning A.J, Thorne P.D., 2015. The pervasive
1153 role of biological cohesion in bedform development. *Nature communications*, 6.
1154 doi: [10.1038/ncomms7257](https://doi.org/10.1038/ncomms7257)

1155 Mantz, P. A. (1978). Bedforms produced by fine, cohesionless, granular and flakey sediments under
1156 subcritical water flows. *Sedimentology*, 25(1), 83-103. DOI: 10.1111/j.1365-3091.1978.tb00302.x

1157 Martin, R. L., Jerolmack, D. J., 2013. Origin of hysteresis in bed form response to unsteady
1158 flows. *Water Resources Research*, 49(3), 1314-1333. DOI: 10.1002/wrcr.20093

1159 Martinius, A. W., and Van den Berg, J. H. 2011. *Atlas of sedimentary structures in estuarine and
1160 tidally-influenced river deposits of the Rhine-Meuse-Scheldt system* (p. 298). EAGE.

1161 McElroy, B., Mohrig, D., 2009. Nature of deformation of sandy bed forms. *Journal of Geophysical
1162 Research: Earth Surface*, 114(F3). DOI: 10.1029/2008JF001220

1163 McLean, S. R., 1990. The stability of ripples and dunes. *Earth-Science Reviews*, 29(1), 131-144.
1164 [https://doi.org/10.1016/0012-8252\(0\)90032-Q](https://doi.org/10.1016/0012-8252(0)90032-Q)

1165 Milan, D. J., Heritage, G. L., Large, A. R. G., and Charlton, M. E., 2001. Stage dependent variability in
1166 tractive force distribution through a riffle–pool sequence. *Catena*, 44(2), 85-109.
1167 [https://doi.org/10.1016/S0341-8162\(00\)00155-7](https://doi.org/10.1016/S0341-8162(00)00155-7)

1168 Nabi, M., Vriend, H. J., Mosselman, E., Sloff, C. J., Shimizu, Y., 2013. Detailed simulation of
1169 morphodynamics: 3. Ripples and dunes. *Water resources research*, 49(9), 5930-5943.
1170 DOI: 10.1002/wrcr.20457

1171 Nabi, M., Kimura, I., Hsu, S. M., Giri, S., Shimizu, Y., 2015. Computational modeling of dissipation and
1172 regeneration of fluvial sand dunes under variable discharges. *Journal of Geophysical Research:
1173 Earth Surface*, 120(7), 1390-1403. DOI: 10.1002/2014JF003364

1174 Naqshband, S., Ribberink, J. S., Hurther, D., and Hulscher, S. J. M. H., 2014a. Bed load and suspended
1175 load contributions to migrating sand dunes in equilibrium. *Journal of Geophysical Research:
1176 Earth Surface*, 119(5), 1043-1063. DOI: 10.1002/2013JF003043

1177 Naqshband, S., Ribberink, J. S., and Hulscher, S. J., 2014b. Using both free surface effect and
1178 sediment transport mode parameters in defining the morphology of river dunes and their
1179 evolution to upper stage plane beds. *Journal of Hydraulic Engineering*, 140(6), 06014010.
1180 [https://doi.org/10.1061/\(ASCE\)HY.1943-7900.0000873](https://doi.org/10.1061/(ASCE)HY.1943-7900.0000873)

1181 Nelson, J. M., McLean, S. R., Wolfe, S. R., 1993. Mean flow and turbulence fields over two-
1182 dimensional bed forms. *Water Resources Research*, 29(12), 3935-3953.
1183 DOI: 10.1029/93WR01932

1184 Nittrouer, J. A., Allison, M. A., Campanella R., 2008. Bedform transport rates for the lowermost
1185 Mississippi River, *J. Geophys. Res.*, 113, F03004, doi:10.1029/2007JF000795.

1186 Nordin, C. F., 1971. *Statistical properties of dune profiles*. Geological Survey Professional Paper No.
1187 562-F.

1188 Omidyeganeh, M., Piomelli, U., 2011. Large-eddy simulation of two-dimensional dunes in a steady,
1189 unidirectional flow. *Journal of Turbulence*, (12), N42.
1190 <http://dx.doi.org/10.1080/14685248.2011.609820>

1191 Omidyeganeh, M., Piomelli, U., 2013a. Large-eddy simulation of three-dimensional dunes in a
1192 steady, unidirectional flow. Part 1. Turbulence statistics. *Journal of Fluid Mechanics*, 721,
1193 454. <https://doi.org/10.1017/jfm.2013.3>

1194 Omidyeganeh, M., Piomelli, U., 2013b. Large-eddy simulation of three-dimensional dunes in a
1195 steady, unidirectional flow. Part 2. Flow structures. *Journal of Fluid Mechanics*, 734, 509-
1196 534. <https://doi.org/10.1017/jfm.2013.499>

1197 Paarlberg, A. J., Dohmen-Janssen, C. M., Hulscher, S. J., Termes, P., 2009. Modeling river dune
1198 evolution using a parameterization of flow separation. *Journal of Geophysical Research: Earth
1199 Surface*, 114(F1). DOI: 10.1029/2007JF000910

1200 Paarlberg, A. J., Dohmen-Janssen, C. M., Hulscher, S. J., Termes, P., and Schielen, R. (2010).
1201 Modelling the effect of time-dependent river dune evolution on bed roughness and stage. *Earth
1202 Surface Processes and Landforms*, 35(15), 1854-1866. DOI: 10.1002/esp.2074

1203 Paola, C., Borgman, L., 1991. Reconstructing random topography from preserved
1204 stratification. *Sedimentology*, 38(4), 553-565. DOI: 10.1111/j.1365-3091.1991.tb01008.x

1205 Parsons, D. R., Best, J. L., Orfeo, O., Hardy, R. J., Kostaschuk, R., Lane, S. N., 2005. Morphology and
1206 flow fields of three-dimensional dunes, Rio Paraná, Argentina: Results from simultaneous
1207 multibeam echo sounding and acoustic Doppler current profiling. *Journal of Geophysical
1208 Research: Earth Surface*, 110(F4). DOI: 10.1029/2004JF000231

1209 Parsons, D. R., Schindler, R. J., Hope, J. A., Malarkey, J., Baas, J. H., Peakall, J., Manning A.J., Ye L.,
1210 Simmons S., Paterson D.M., Aspden. R.J., Bass, S.J., Davies, A.G., Lichtman, I.D., Thorne, P.D.,
1211 2016. The role of biophysical cohesion on subaqueous bed form size. *Geophysical research
1212 letters*, 43(4), 1566-1573. DOI: 10.1002/2016GL067667

1213 Pretious, E. S., & Blench, T., 1951. Final report on special observations on bed movement in the
1214 lower Fraser River at Ladner Reach During the 1950 freshet. *National Research Council of
1215 Canada*.

1216 Raudkivi, A. J., Witte, H. H., 1990. Development of bed features. *Journal of Hydraulic
1217 Engineering*, 116(9), 1063-1079. [https://doi.org/10.1061/\(ASCE\)0733-9429\(1990\)116:9\(1063\)](https://doi.org/10.1061/(ASCE)0733-9429(1990)116:9(1063))

1218 Reesink, A. J. H., Bridge, J. S., 2007. Influence of superimposed bedforms and flow unsteadiness on
1219 formation of cross strata in dunes and unit bars. *Sedimentary Geology*, 202(1), 281-296.
1220 <https://doi.org/10.1016/j.sedgeo.2007.02.005>

1221 Reesink, A. J., Bridge, J. S., 2009. Influence of bedform superimposition and flow unsteadiness on the
1222 formation of cross strata in dunes and unit bars—Part 2, further experiments. *Sedimentary*
1223 *Geology*, 222(3), 274-300. <https://doi.org/10.1016/j.sedgeo.2009.09.014>

1224 Reesink, A. J., Bridge, J. S., 2011. Evidence of bedform superimposition and flow unsteadiness in unit-
1225 bar deposits, South Saskatchewan River, Canada. *Journal of Sedimentary Research*, 81(11), 814-
1226 840. doi: 10.2110/jsr.2011.69

1227 Reesink A.J.H., Ashworth P.J. Sambrook Smith G.H., Best J.L., Parsons D.R., Amsler M.L., Hardy R.J.,
1228 Lane S.N., Nicholas A.P., Orfeo O.O., Sandbach S.D., Simpson C.J., Szupiany R.N., 2014. Scales and
1229 causes of heterogeneity in bars in a large multi-channel river: Río Paraná, Argentina.
1230 *Sedimentology*, 61(4), p. 1055-1085. DOI: 10.1111/sed.12092

1231 Reesink A.J.H., Parsons D.R., Thomas R.E., 2014. *Sediment transport and bedform development in the*
1232 *lee of bars: Evidence from fixed- and partially-fixed bed experiments*. River Flow 2014,
1233 Conference Proceedings

1234 Reesink, A. J. H., Van den Berg, J. H., Parsons, D. R., Amsler, M. L., Best, J. L., Hardy, R. J., Szupiany, R.
1235 N., 2015. Extremes in dune preservation: Controls on the completeness of fluvial deposits. *Earth-*
1236 *Science Reviews*, 150, 652-665. <https://doi.org/10.1016/j.earscirev.2015.09.008>

1237 Reesink A.J.H., Parsons D.R., Ashworth P.J., Best J.L., Darby S.E., Hardy R.J., 2016. Visualising dune
1238 deformation and sediment dispersal across dune fields. Proceedings of the Marine and River
1239 Dunes conference 2016

1240 Rennie, C. D., Millar, R. G., & Church, M. A., 2002. Measurement of bed load velocity using an
1241 acoustic Doppler current profiler. *Journal of Hydraulic Engineering*, 128(5), 473-483.
1242 [https://doi.org/10.1061/\(ASCE\)0733-9429\(2002\)128:5\(473\)](https://doi.org/10.1061/(ASCE)0733-9429(2002)128:5(473))

1243 Rodrigues, S., Mosselman, E., Claude, N., Wintenberger, C. L., Juge, P., 2015. Alternate bars in a
1244 sandy gravel bed river: generation, migration and interactions with superimposed dunes. *Earth*
1245 *Surface Processes and Landforms*, 40(5), 610-628. DOI: 10.1002/esp.3657

1246 Rubin, D. M., McCulloch, D. S., 1980. Single and superimposed bedforms: a synthesis of San
1247 Francisco Bay and flume observations. *Sedimentary Geology*, 26(1-3), 207-231.
1248 [https://doi.org/10.1016/0037-0738\(80\)90012-3](https://doi.org/10.1016/0037-0738(80)90012-3)

1249 Saunderson, H. C., and Lockett, F. P., 1983. Flume experiments on bedforms and structures at the
1250 dune-plane bed transition. In *Modern and Ancient Fluvial Systems* (Vol. 6, pp. 49-58).
1251 International Association of Sedimentologists.

1252 Schatz, V., and Herrmann, H. J., 2006. Flow separation in the lee side of transverse dunes: a
1253 numerical investigation. *Geomorphology*, 81(1), 207-216.
1254 <https://doi.org/10.1016/j.geomorph.2006.04.009>

1255 Schindler, R.J., Parsons, D.R., Ye, L., Hope, J.A., Baas J.H., Peakall, J., Manning, A.J., Aspden, R.J.,
1256 Malarkey, J., Simmons, S., Paterson, D.M., Lichtman, I.D., Davies, A.G., Thorne, P.D., Bass S.J.,
1257 Sticky stuff: Redefining bedform prediction in modern and ancient environments. *Geology* 2015;
1258 43 (5): 399-402. doi: 10.1130/G36262.1

1259 Schmeeckle, M. W., 2014. Numerical simulation of turbulence and sediment transport of medium
1260 sand. *Journal of Geophysical Research: Earth Surface*, 119(6), 1240-1262.
1261 DOI: 10.1002/2013JF002911

1262 Schmeeckle, M. W., 2015. The role of velocity, pressure, and bed stress fluctuations in bed load
1263 transport over bed forms: numerical simulation downstream of a backward-facing step. *Earth*
1264 *Surface Dynamics*, 3(1), 105. doi:10.5194/esurf-3-105-2015

1265 Schumm, S. A., 1977. *The fluvial system*. John Wiley and Sons, New York. 338p.

1266 Schumm, S. A., 1998. *To Interpret the Earth: Ten ways to be wrong*. Cambridge University Press.
1267 133p.

1268 Sear, D. A. (1996). Sediment transport processes in pool–riffle sequences. *Earth Surface Processes*
1269 *and Landforms*, 21(3), 241-262. DOI: 10.1002/(SICI)1096-9837(199603)21:3<241::AID-
1270 ESP623>3.0.CO;2-1

1271 Shimizu, Y., Giri, S., Yamaguchi, S., & Nelson, J., 2009. Numerical simulation of dune–flat bed
1272 transition and stage-discharge relationship with hysteresis effect. *Water Resources*
1273 *Research*, 45(4). DOI: 10.1029/2008WR006830

1274 Simons, D. B., Richardson, E. V., 1966. *Resistance to flow in alluvial channels* (p. 61). Geological
1275 Survey Professional Paper 422-J, Washington, DC: US Government Printing Office.

1276 Smith, B. T., and R. Ettema (1997), Ice-cover influence on flow structure over dunes Ice-cover
1277 influence on flow structure over dunes, *J. Hydraulic Research*, 35(5), 37–41.

1278 Szupiany, R. N., Amsler, M. L., Hernandez, J., Parsons, D. R., Best, J. L., Fornari, E., and Trento, A.
1279 2012. Flow fields, bed shear stresses, and suspended bed sediment dynamics in bifurcations of a
1280 large river. *Water Resources Research*, 48(11). DOI: 10.1029/2011WR011677

1281 Ten Brinke, W. B. M., Wilbers, A. W. E., and Wesseling, C. 1999. Dune Growth, Decay and Migration
1282 Rates during a Large-Magnitude Flood at a Sand and Mixed Sand–Gravel Bed in the Dutch Rhine
1283 River System. *Fluvial sedimentology VI*, 15-32. DOI: 10.1002/9781444304213.ch2

1284 Thomas, N., B. Davidsson, M. R. El-Maarry, S. Fornasier, L. Giacomini, A. G. Gracia-Berná, S. F. Hviid,
1285 W.-H. Ip, L. Jorda, H. U. Keller, J. Knollenberg, E. Kührt, F. La Forgia, I. L. Lai, Y. Liao, R. Marschall,
1286 M. Massironi, S. Mottola, M. Pajola, O. Poch, A. Pommerol, F. Preusker, F. Scholten, C. C. Su, J. S.
1287 Wu, J.-B. Vincent, H. Sierks, C. Barbieri, P. L. Lamy, R. Rodrigo, D. Koschny, H. Rickman, M. F.
1288 A’Hearn, M. A. Barucci, J.-L. Bertaux, I. Bertini, G. Cremonese, V. Da Deppo, S. Debei, M. de
1289 Cecco, M. Fulle, O. Groussin, P. J. Gutierrez, J.-R. Kramm, M. Küppers, L. M. Lara, M. Lazzarin, J. J.
1290 Lopez Moreno, F. Marzari, H. Michalik, G. Naletto, J. Agarwal, C. Güttler, N. Oklay C. Tubiana
1291 Knollenberg, J., 2015. Redistribution of particles across the nucleus of comet 67P/Churyumov-
1292 Gerasimenko. *Astronomy and Astrophysics*, 583, A17. doi:10.1051/0004-6361/201526049.

1293 Tuijnder, A. P., Ribberink, J. S., Hulscher, S. J., 2009. An experimental study into the geometry of
1294 supply-limited dunes. *Sedimentology*, 56(6), 1713-1727. DOI: 10.1111/j.1365-3091.2009.01054.x

1295 Unsworth, C.A., Parsons, D.R., Hardy, R.J., Reesink, A.J.H., Best, J.L., Ashworth, P.J., and Keevil, G.M.
1296 In press. The impact of non-equilibrium flow on the structure of turbulence over river dunes.
1297 *Water Resources Research*

1298 Van den Berg, J.H., Van Gelder, A. 1993. A new bedform stability diagram, with emphasis on the
1299 transition of ripples to plane bed in flows over fine sand and silt. *Alluvial Sedimentation (Special*
1300 *Publication 17 of the IAS)*,66, 11.

1301 Van der Mark, C. F., Blom, A., and Hulscher, S. J. M. H., 2008. Quantification of variability in bedform
1302 geometry. *Journal of Geophysical Research: Earth Surface*, 113(F3). DOI: 10.1029/2007JF000940

1303 Van Rijn, L. C., 1984. Sediment transport, part III: bed forms and alluvial roughness. *Journal of*
1304 *hydraulic engineering*, 110(12), 1733-1754. [https://doi.org/10.1061/\(ASCE\)0733-](https://doi.org/10.1061/(ASCE)0733-9429(1984)110:12(1733))
1305 [9429\(1984\)110:12\(1733\)](https://doi.org/10.1061/(ASCE)0733-9429(1984)110:12(1733))

1306 Van Rijn, L. C., 1993. Principles of sediment transport in rivers, estuaries and coastal seas (Vol. 1006).
1307 Amsterdam: Aqua publications.

1308 Venditti, J. G., Church, M., and Bennett, S. J., 2005a. Morphodynamics of small-scale superimposed
1309 sand waves over migrating dune bed forms. *Water resources research*, 41(10).
1310 DOI: 10.1029/2004WR003461

1311 Venditti, J. G., Church, M., and Bennett, S. J., 2005b. On the transition between 2D and 3D
1312 dunes. *Sedimentology*, 52(6), 1343-1359. DOI: 10.1111/j.1365-3091.2005.00748.x

1313 Venditti, J. G., Lin, C. Y. M., and Kazemi, M., 2016. Variability in bedform morphology and kinematics
1314 with transport stage. *Sedimentology* 63, 1017-1039. DOI: 10.1111/sed.12247

1315 Wan, Z., Wang, Z., 1994. Hyperconcentrated Flow. In: Balkema, A.A. (Ed.) Brookfield, VT, p. 290.

1316 Warmink, J. J., Straatsma, M. W., Huthoff, F., Booij, M. J., and Hulscher, S. J. M. H., 2013. Uncertainty
1317 of design water levels due to combined bed form and vegetation roughness in the Dutch River
1318 Waal. *Journal of flood risk management*, 6(4), 302-318.

1319 Warmink, J. J., Dohmen-Janssen, C. M., Lansink, J., Naqshband, S., Duin, O. J., Paarlberg, A. J.,
1320 Termes, P., Hulscher, S. J. 2014. Understanding river dune splitting through flume experiments
1321 and analysis of a dune evolution model. *Earth surface processes and landforms*, 39(9), 1208-
1322 1220. DOI: 10.1002/esp.3529

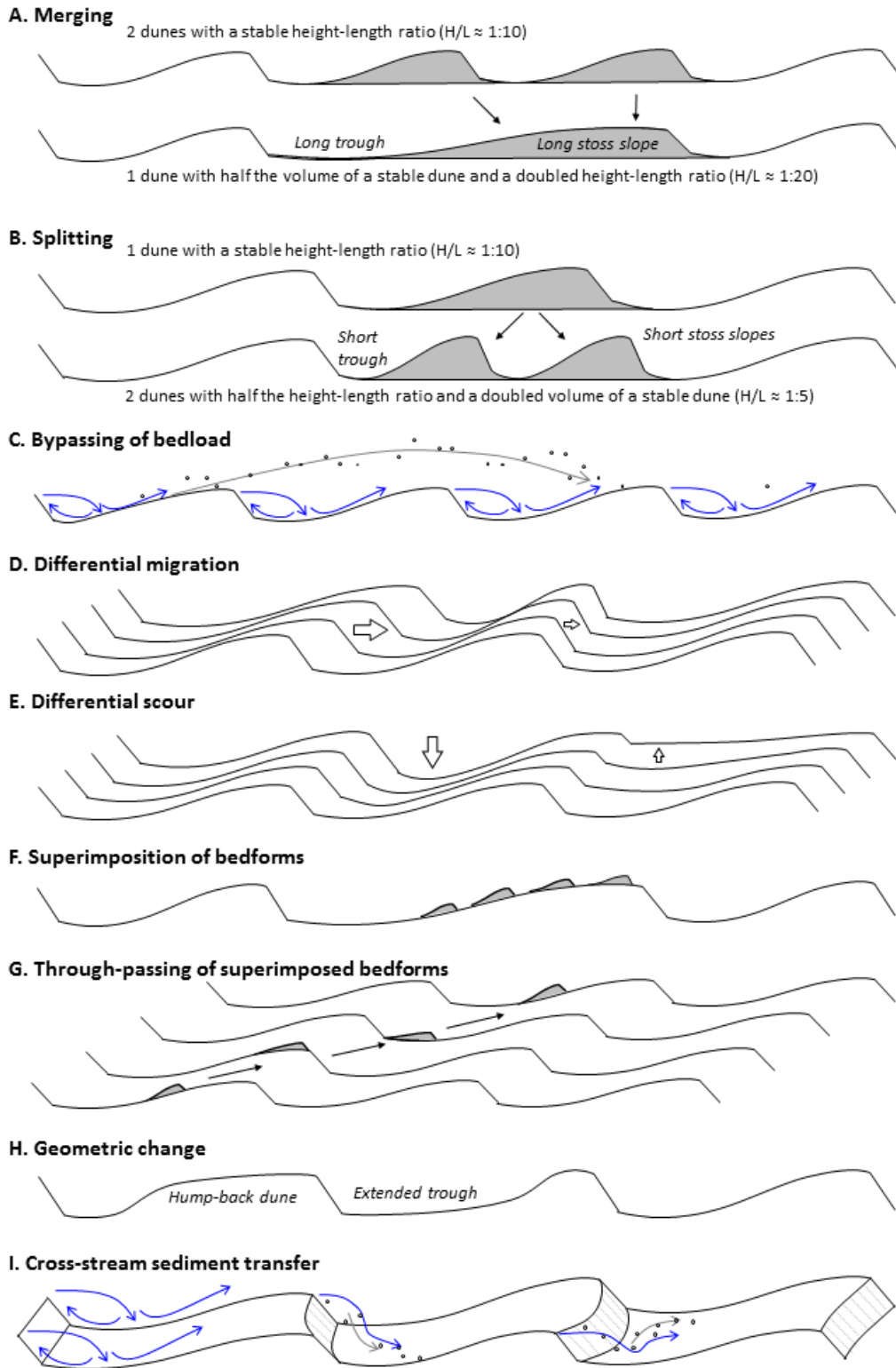
1323 Warmink, J. J., 2014. Dune dynamics and roughness under gradually varying flood waves, comparing
1324 flume and field observations. *Advances in geosciences*, 39, 115-121. doi:10.5194/adgeo-39-115-
1325 2014

1326 Werner, B. T., and Kocurek, G., 1997. Bed-form dynamics: Does the tail wag the dog? *Geology*, 25(9),
1327 771-774. [https://doi.org/10.1130/0091-7613\(1997\)025<0771:BFDDTT>2.3.CO;2](https://doi.org/10.1130/0091-7613(1997)025<0771:BFDDTT>2.3.CO;2)

1328 Werner, B. T., and Kocurek, G., 1999. Bedform spacing from defect dynamics. *Geology*, 27(8), 727-
1329 730. [https://doi.org/10.1130/0091-7613\(1999\)027<0727:BSFDD>2.3.CO;2](https://doi.org/10.1130/0091-7613(1999)027<0727:BSFDD>2.3.CO;2)

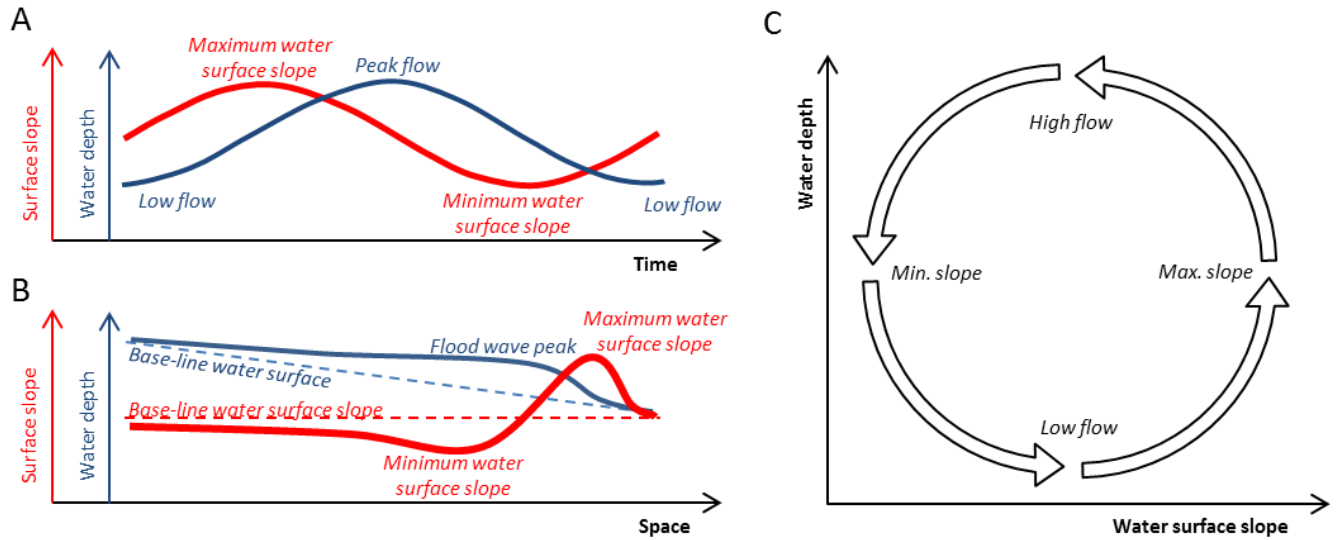
1330 Wilbers, A. W. E., Ten Brinke, W. B. M., 2003. The response of subaqueous dunes to floods in sand
1331 and gravel bed reaches of the Dutch Rhine. *Sedimentology*, 50(6), 1013-1034.
1332 DOI: 10.1046/j.1365-3091.2003.00585.x

1333 Yalin M.S., 1964. Geometrical properties of sand waves. *Journal of the Hydraulics Division*, American
1334 Society of Civil Engineers 90(5), 105-119.
1335
1336
1337
1338



1339
 1340
 1341
 1342
 1343

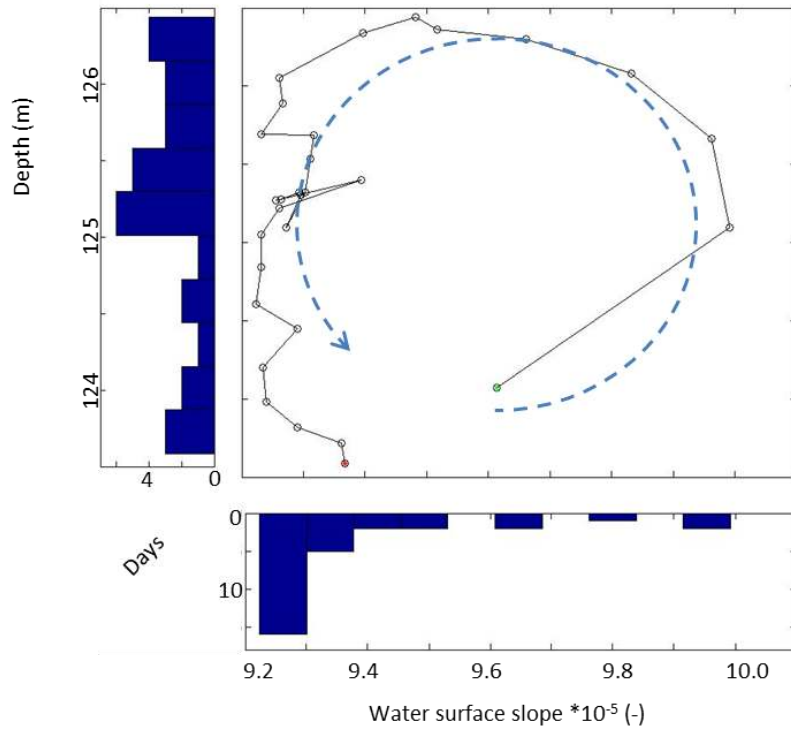
Figure 1. A-B The generation of local sources and sinks of sediment within a dune field by merging and splitting of dunes. C-I Sediment transport processes that may contribute to the dispersal of sediment across a dune field. Blue arrows indicate flow paths and directions.



1344
 1345
 1346
 1347
 1348
 1349

Figure 2. Depth and water-surface slope associated with flood waves is out-of-phase over time and in space, as illustrated here for: A) a simple symmetrical wave at a point over time, and B) for a single time along the length of a non-tidal river. C) The out-of-phase relation between depth and slope creates a cycle in depth and slope that is repeated for successive floods.

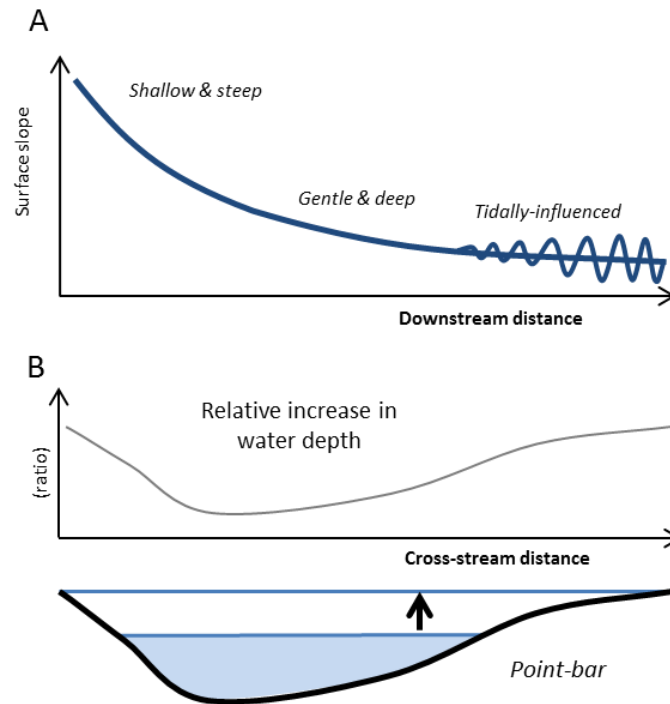
1350



1351
1352
1353
1354
1355
1356
1357
1358
1359

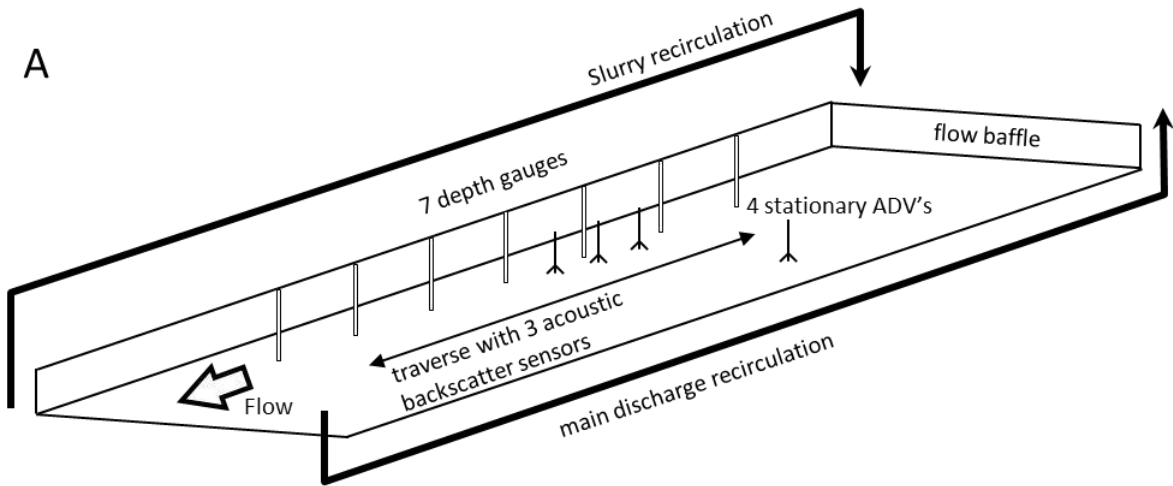
Figure 3. Water depth and water surface slope in the Mississippi River between the gauging stations at Saint Louis, MO and Chester, IL (data from USGS Water Information System). The distance between these stations is 114 km, and the average elevation difference is 10.7 m. The velocity of the flood wave was 171 km/day, and the flood lasted for approximately 30 days. The data show that the out-of-phase relation between depth and slope is significant for non-tidal rivers. The larger number of days during which the water depth is high and water-surface slope is decreasing (top left corner, waning flood stage) may bias observations of hydraulic conditions and corresponding dune behaviour in natural rivers.

1360



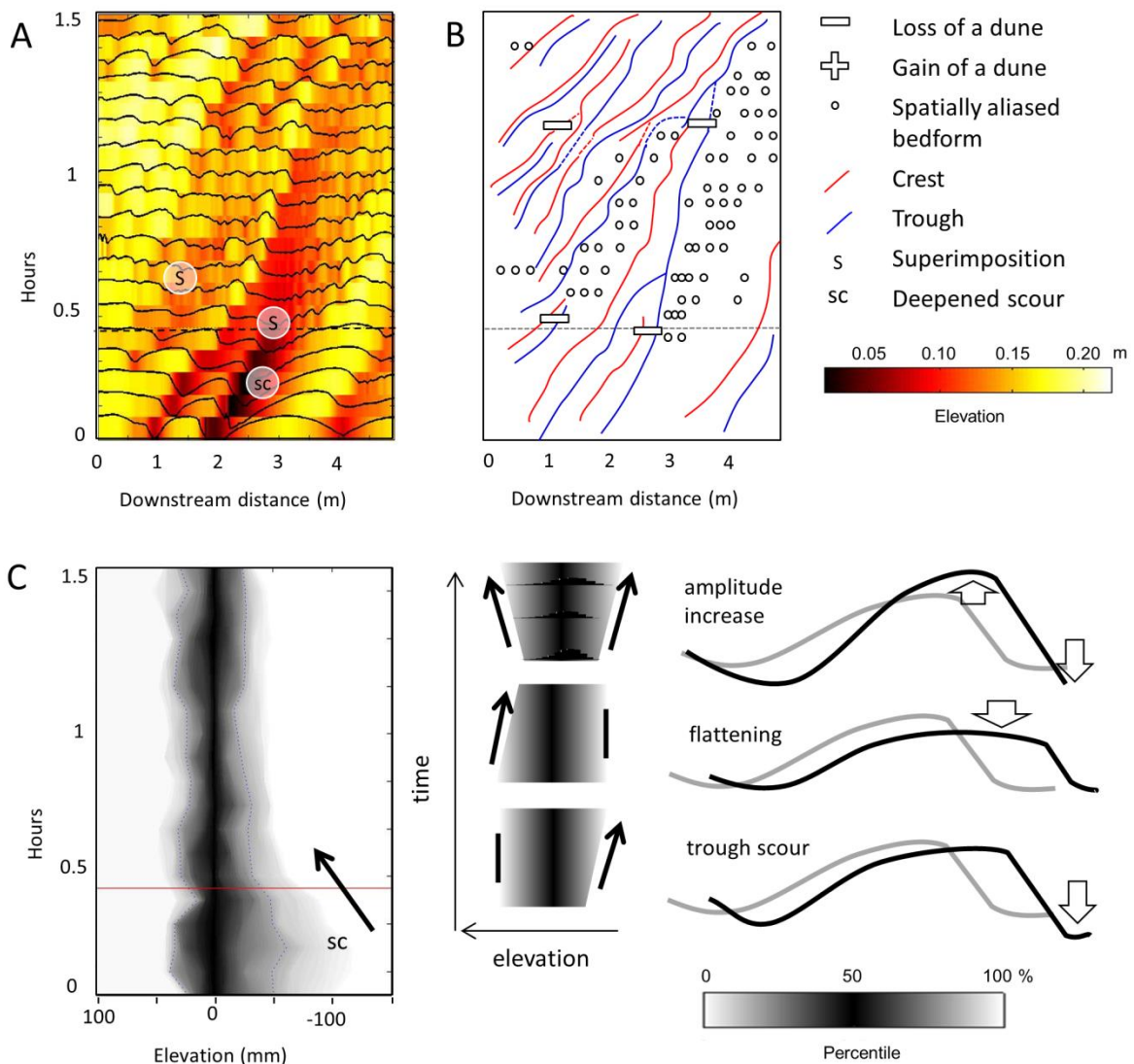
1361
1362
1363
1364
1365
1366

Figure 4. The magnitude of changes in flow depth and water-surface slope vary spatially: A) along a river within a catchment from shallow and steep upland streams, to deep and low-gradient lowland rivers to tidally-influenced rivers, and, B) locally across the channel from the thalweg to the bar tops. The relative change in water depth is very large on bar flanks and bar tops.



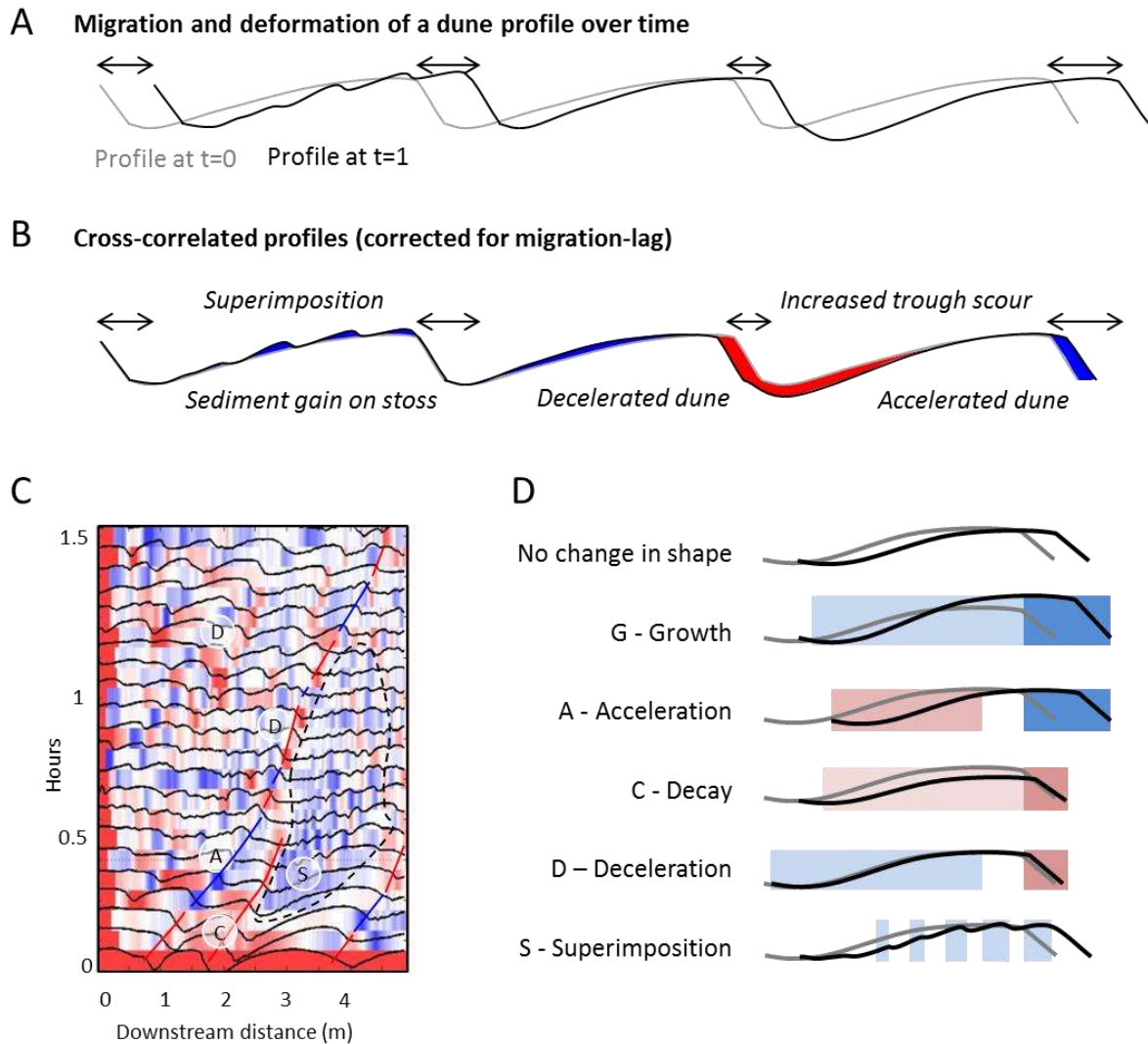
1368
1369
1370
1371
1372

Figure 5. A) Diagram of the experimental set-up and B) photograph of the drained flume bed, looking upstream.



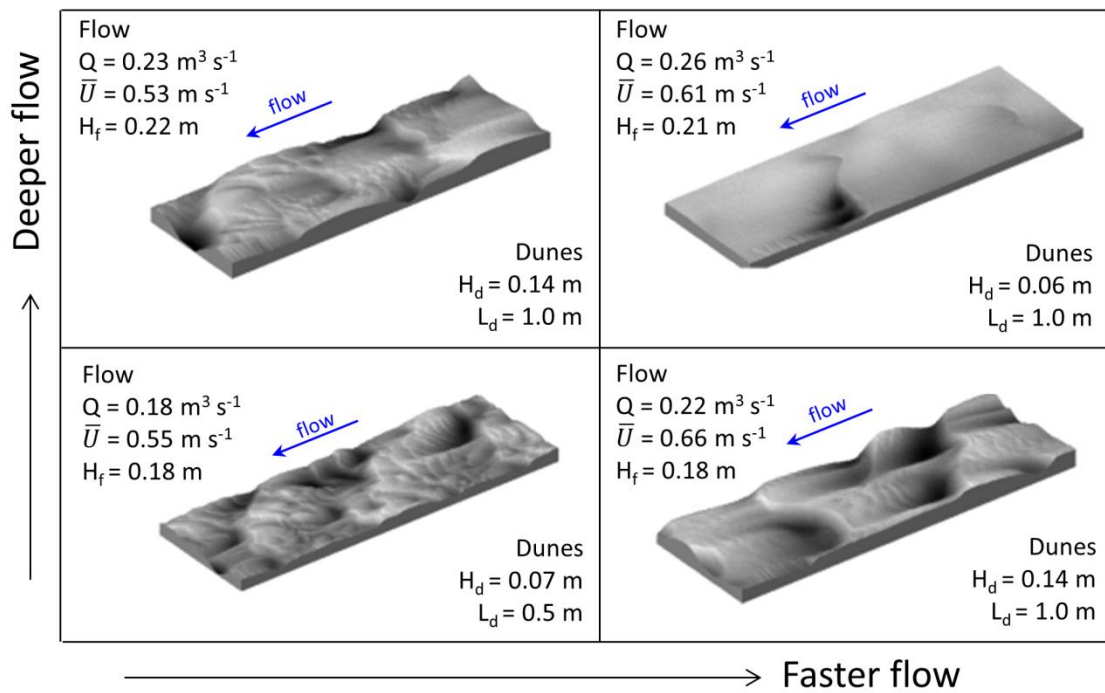
1373
 1374
 1375
 1376
 1377
 1378
 1379
 1380
 1381

Figure 6. A) Dune profiles over time (cf. Raudkivi and Witte, 1990) and for change in conditions (Table 2). The changes in flow are imposed at 0.5 h. B) The kinematic interpretation associated with A. The example (Table 2) illustrates the presence of trains of superimposed bedforms following the loss of two dunes. The dune profiles and kinematic analyses of all 23 stage changes are given in Figures 9 and 11. C) Temporal development of the distribution of the bed elevation illustrates that changes in the elevation of troughs and crests are commonly out-of-phase. The red line indicates the time of the imposed change in flow. The analysis of bed elevations in all 23 stage changes is given in Figure 13.



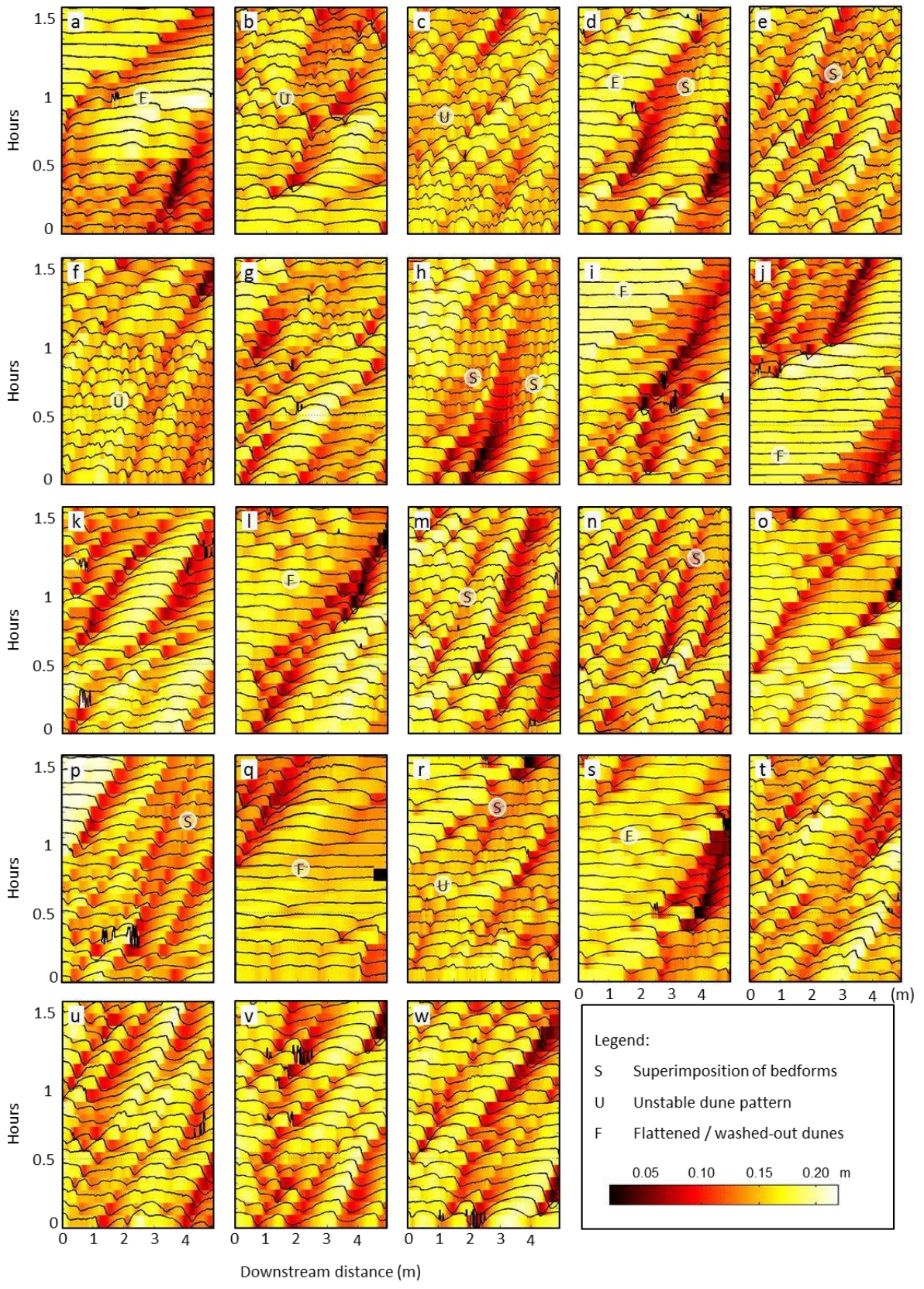
1382
1383
1384
1385
1386
1387
1388
1389

Figure 7. A-B) The residuals of a dune profile cross-correlation analysis (cf. McElroy and Mohrig, 2009) visualise local gain and loss of sediment within a mobile dune field. C-D) when plotted over time, different signatures indicate different processes (see also Fig. 2). Red and blue lines in (C) indicate the relative loss and gain of sediment from lee slopes respectively. The dashed black line in C outlines a zone with a dominant gain of sediment.



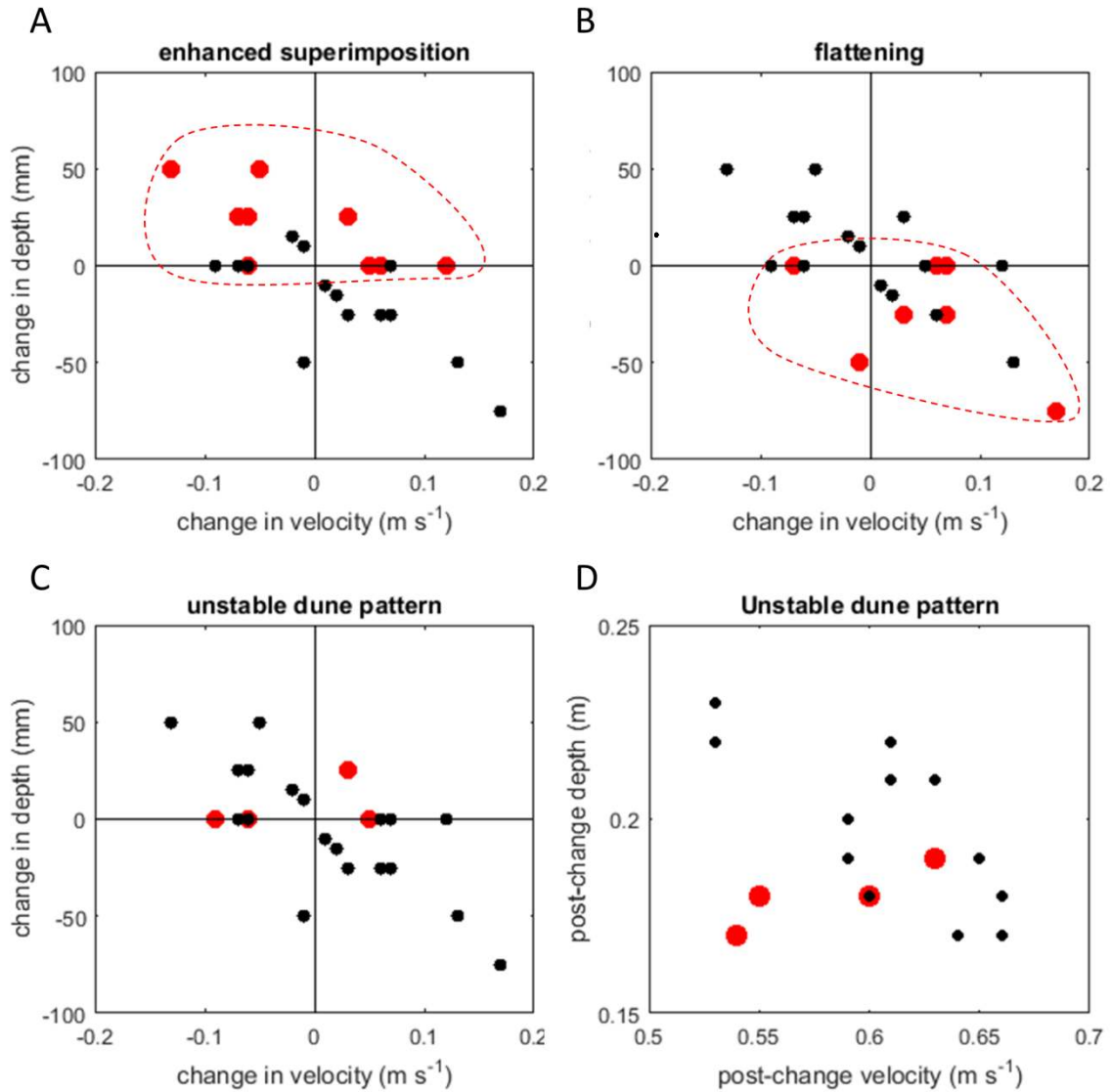
1390
 1391
 1392
 1393

Figure 8. Scanned sections of four dune beds 3 m long and 1 m wide, associated with conditions 3, 11, 17, and 24 (see Table 1). Different dune morphology is observed for different conditions, which implies that dunes must adapt to imposed changes in flow velocity and depth.

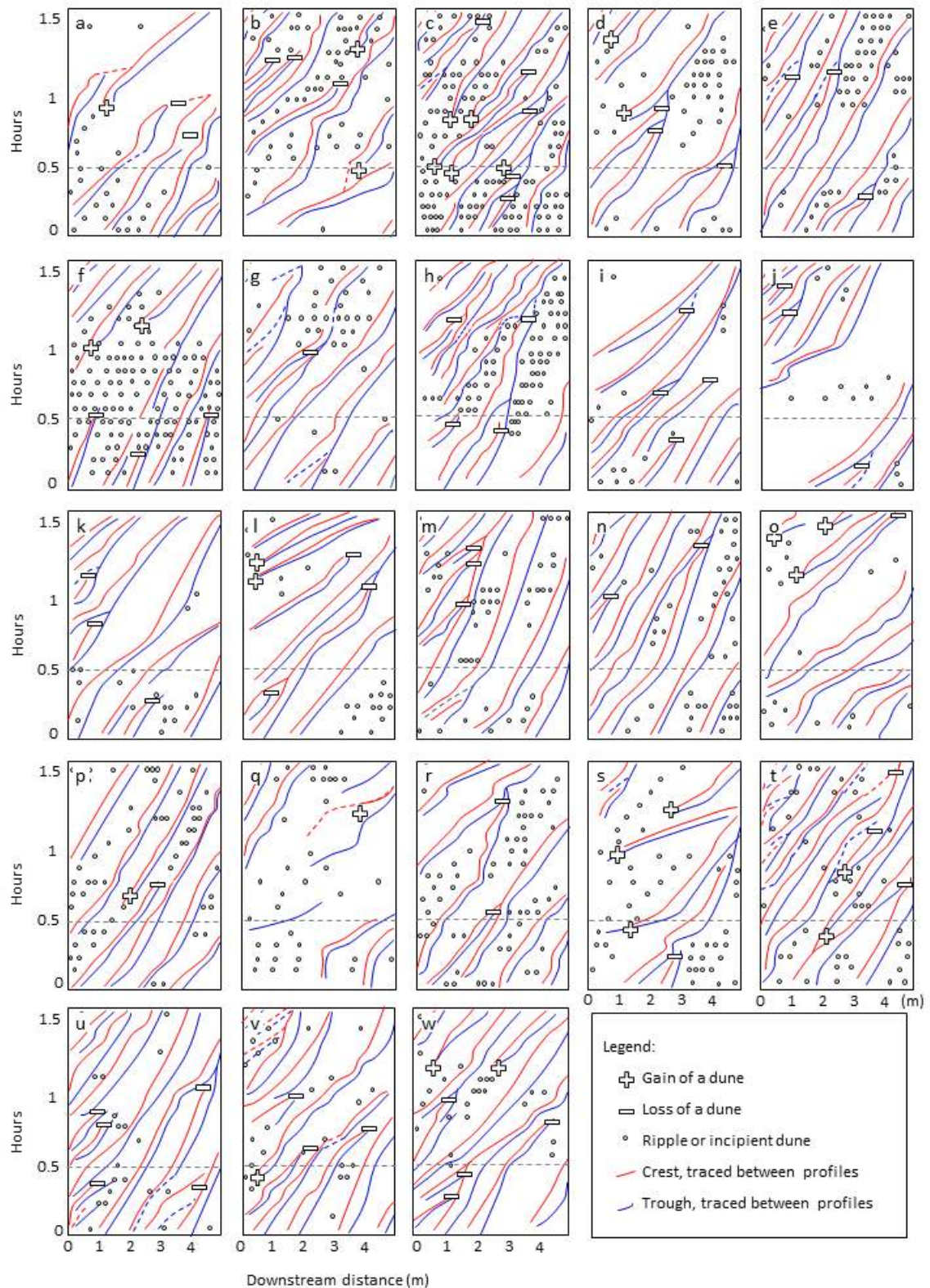


1394
 1395
 1396
 1397
 1398
 1399

Figure 9. Consecutive bed elevation profiles plotted over time and coloured by bed elevation that illustrate the development of the dunes and superimposed bedforms. A-W correspond to the step-wise changes in flow detailed in Table 2. The profiles depict bed profiles 30 minutes prior to the change and 1 hour post-change conditions.

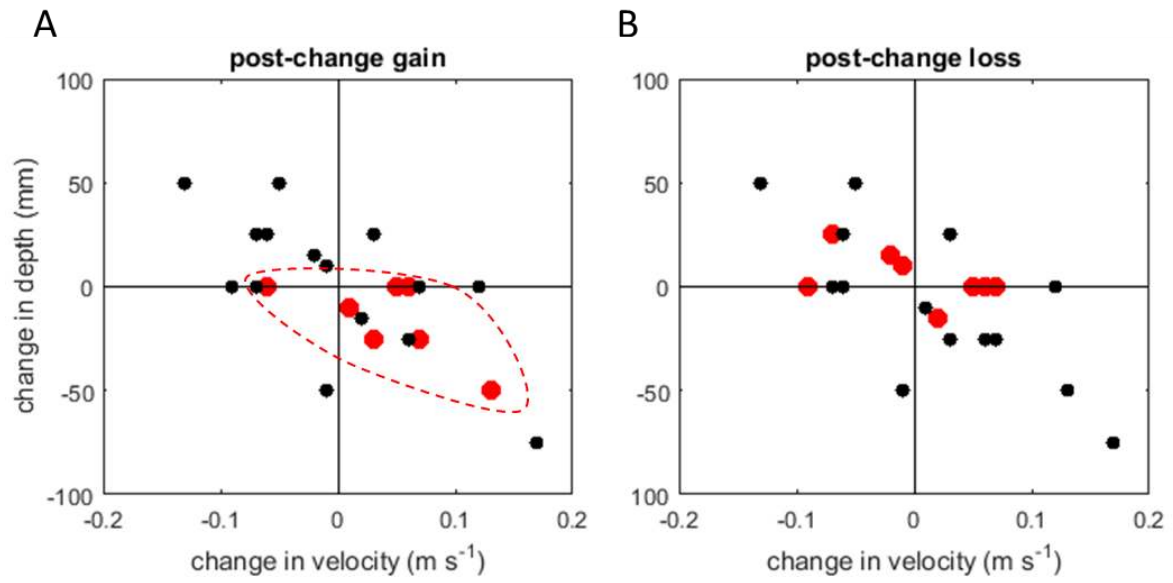


1400
 1401 **Figure 10.** Scatterplots illustrating the preferential occurrence of processes among all experimental
 1402 conditions: A) The development of trains of superimposed bedforms; B) the flattening of dunes; C)
 1403 instability of the dune pattern plotted against the change in depth and velocity; D) instability of the
 1404 dune pattern plotted against the post-change water depth and flow velocity (red = morphological
 1405 response is observed, black = all data). The clustering of observations of superimposition and
 1406 flattening within the plots indicates a dependency on the direction of changes in flow depth and
 1407 velocity. Superimposition is more common when flow depth is increased, whereas flattening of the
 1408 dune profile is most common when flow velocity is increased or flow depth is decreased.
 1409



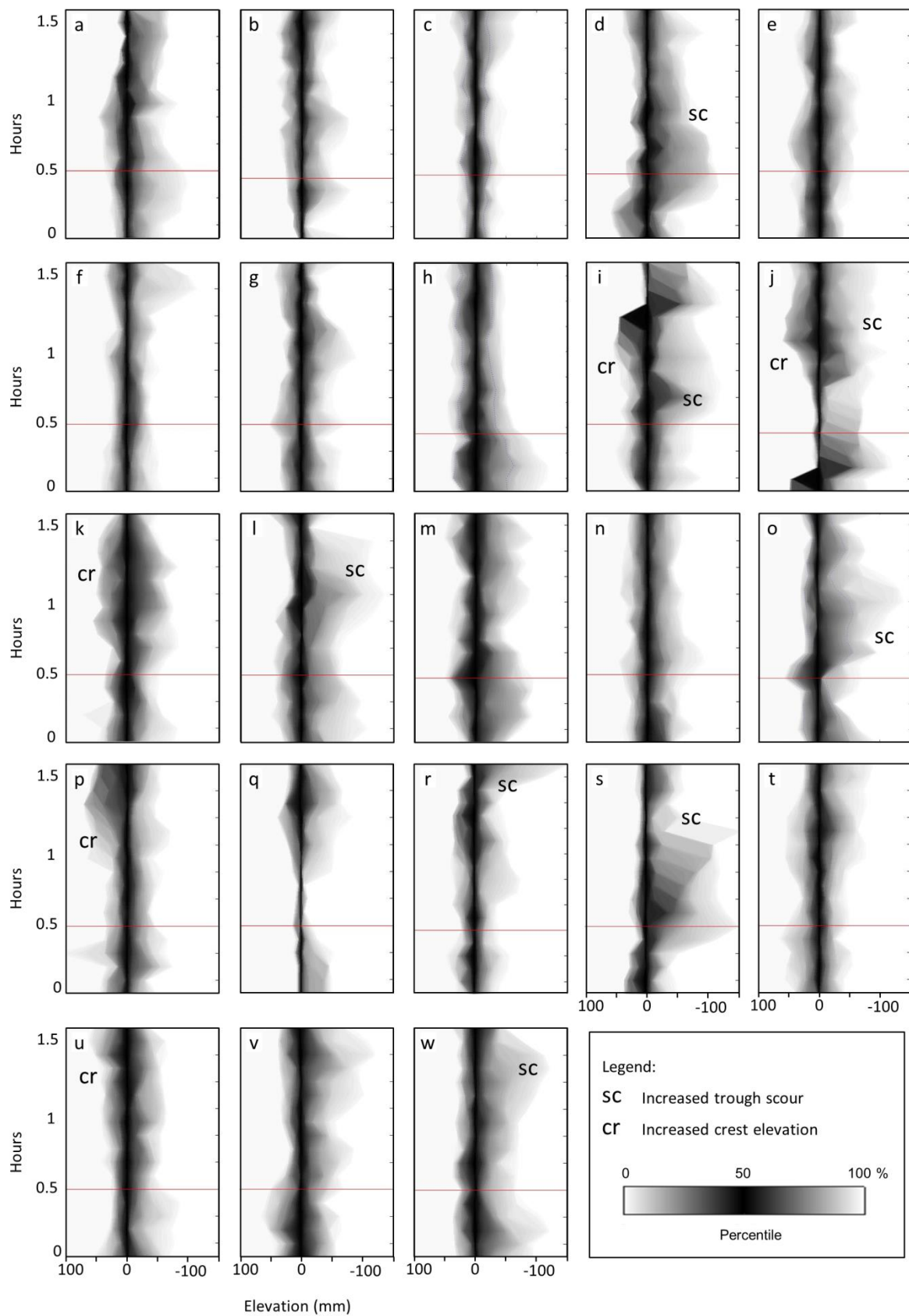
1410
 1411
 1412
 1413
 1414
 1415

Figure 11. Kinematic interpretation of Figure 8: red and blue lines indicate crests and troughs of the dunes respectively, circles indicate bedform crests that could not reliably be traced between profiles, + and - symbols indicate gain and loss of dunes. a-w correspond to the step-wise changes in flow in Table 2. The profiles include 30 minutes prior to the change and 1-hour post-change conditions.



1416
 1417
 1418
 1419

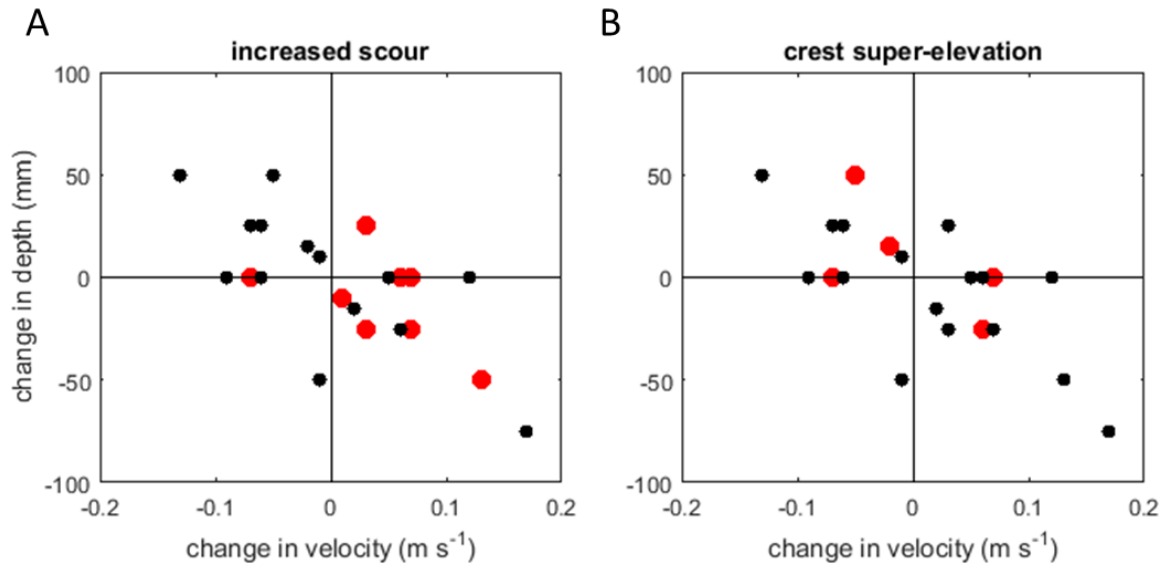
Figure 12. A) Addition of dunes to the dune profile, B) loss of dunes from the dune profile plotted against the water depth and flow velocity (red = morphological change is observed, black = all data).



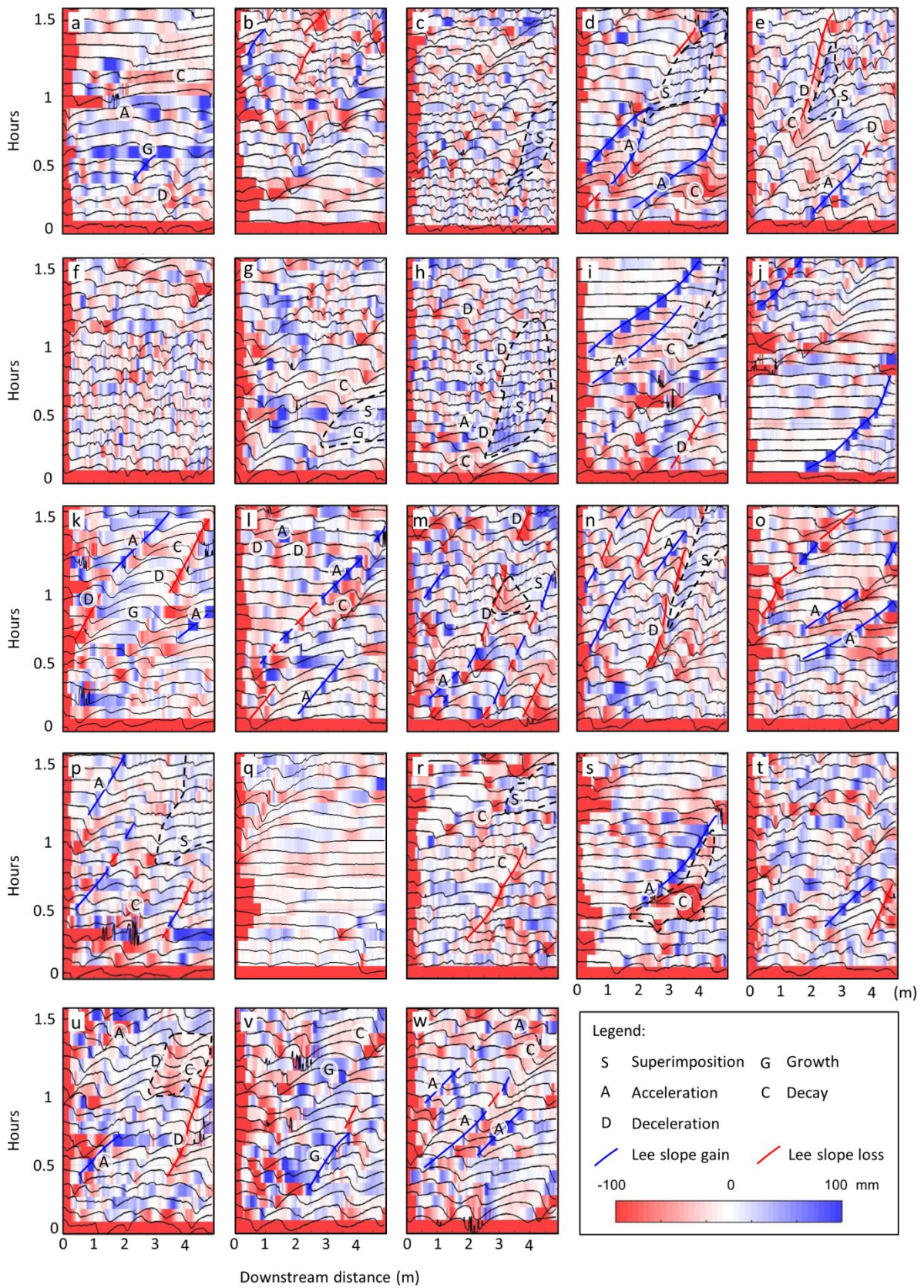
1420
 1421
 1422
 1423

Figure 13. Distributions of the bed elevation in the 5 m long test section centred around the median. a-w correspond to the stepwise changes in flow detailed in Table 2. Each time-slice represents a bed-elevation distribution, coloured from 0% (white), to the median (black), to 100% of the data. *sc*

1424 indicates enhanced scour, *cr* indicates an increase in the elevation of the crest. Note that the
1425 elevation distribution typically develops in an asymmetrical manner.



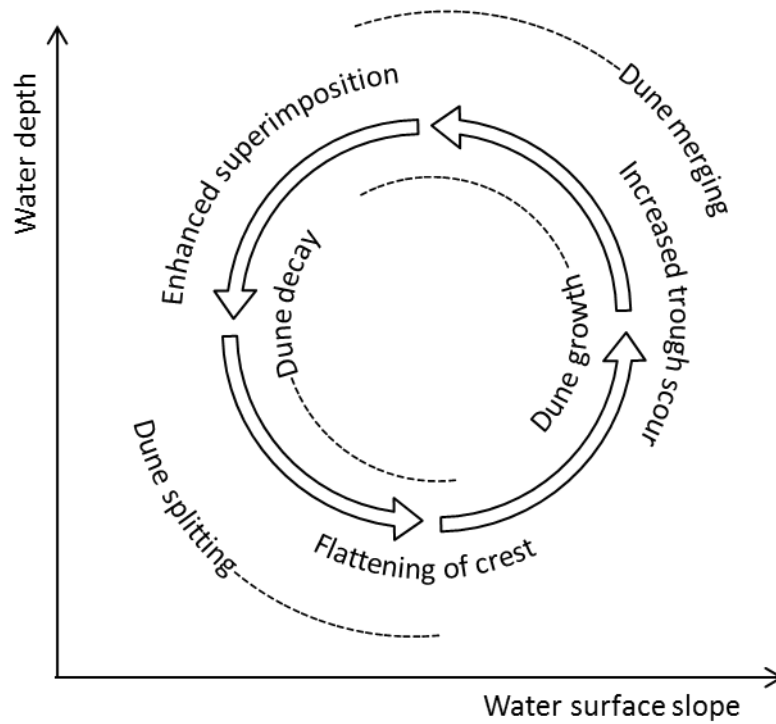
1426
1427 **Figure 14.** A) The increase of scour and B) super-elevation of dune crests above the remaining
1428 profiles as identified from the bed elevation distributions, and plotted as a function of water depth
1429 and flow velocity (red = morphological change is observed, black = all data). Note that increased
1430 scour is mostly observed under the higher velocities, and super-elevation of the crest is mostly
1431 observed in the deeper flows.
1432



1433
 1434
 1435
 1436

Figure 15. Consecutive profiles coloured by deformation (see also Fig. 7A-B). Note that zones of increased erosion and deposition relative to the mean profile shift persist over time: this indicates that some dunes systematically attract sediment whereas others systematically shed sediment.

1437 Trains of superimposed bedforms appear systematically on stoss slopes that attract sediment
1438 (decreased migration of the stoss relative to the mean dune migration).
1439
1440
1441
1442
1443



1444 **Figure 16.** Conceptual model of expected changes in dune adaptation processes during a flood wave for the
1445 thalweg of a medium-sized river, based on the present experiments with shallow, unidirectional flows (depth
1446 0.17-0.25 m). The nature of this conceptual model will require adaptation for different geomorphological
1447 settings, such as locations with different grain sizes, strong secondary currents, deep flows, or multidirectional
1448 flows.
1449

1450
1451
1452
1453

1454
1455

Table 1. Overview of the 24 investigated flow conditions. Q is discharge, H_f is flow depth, \bar{U} is depth-average velocity, Fr is Froude number, H_d is average dune height, L_d is average dune length.

	Q ($m^3 s^{-1}$)	H_f (m)	\bar{U} ($m s^{-1}$)	Fr	H_d (m)	L_d (m)
1	0.22	0.25	0.46	0.3	0.11	1.0
2	0.212	0.17	0.64	0.49	0.09	1.3
3	0.182	0.18	0.55	0.42	0.07	0.5
4	0.2	0.18	0.6	0.46	0.16	1.3
5	0.22	0.18	0.66	0.5	0.12	1.0
6	0.2	0.18	0.6	0.46	0.08	0.7
7	0.18	0.17	0.54	0.41	0.14	1.1
8	0.22	0.18	0.66	0.5	0.18	1.2
9	0.228	0.23	0.53	0.36	0.14	1.0
10	0.26	0.22	0.61	0.41	0.19	1.6
11	0.228	0.22	0.53	0.36	0.14	1.0
12	0.224	0.19	0.59	0.42	0.14	1.3
13	0.22	0.18	0.66	0.5	0.19	1.1
14	0.224	0.20	0.59	0.42	0.12	1.1
15	0.228	0.22	0.53	0.36	0.14	1.1
16	0.22	0.17	0.66	0.5	0.18	0.9
17	0.26	0.21	0.61	0.41	0.06	1.0
18	0.2	0.18	0.6	0.46	0.08	0.7
19	0.24	0.19	0.63	0.45	0.11	1.2
20	0.22	0.18	0.66	0.5	0.11	1.0
21	0.23	0.19	0.65	0.49	0.14	1.1
22	0.24	0.21	0.63	0.45	0.17	1.1
23	0.23	0.19	0.65	0.49	0.17	0.9
24	0.22	0.18	0.66	0.5	0.14	1.0

1456
1457

Table 2. Overview of the 23 step changes and the observed post-change morphodynamic responses

Step-change nr	stages	Change in flume discharge dQ (m ³ s ⁻¹)	Change in mean velocity dU (m s ⁻¹)	Change in mean water depth dH _l (m)	post-change velocity (m s ⁻¹)	post-change depth (m)	trains of superimposed ripples	unstable pattern	flattening	Number of dunes gained	Number of dunes lost	Increased scour	crest super-elevation	acceleration	deceleration	growth	decay
a	1-2	-0.008	0.17	-0.75	0.64	0.17			y	1	2			y		y	y
b	2-3	-0.03	-0.09	0	0.55	0.18		y		1	3						
c	3-4	0.018	0.05	0	0.6	0.18	y	y		2	3						
d	4-5	0.02	0.06	0	0.66	0.18	y		y	2	3	Y		y			
e	5-6	-0.02	-0.06	0	0.6	0.18	y			2	2				y		y
f	6-7	-0.02	-0.06	0	0.54	0.17		y		2	2						
g	7-8	0.04	0.12	0	0.66	0.18	y			0	1					y	y
h	8-9	0.008	-0.13	0.50	0.53	0.23	y			0	2			y	y		
i	9-10	0.032	0.07	0	0.61	0.22			y	0	3	Y	Y	y			y
j	10-11	-0.032	-0.07	0	0.53	0.22			y	0	2	Y	Y				
k	11-12	-0.004	0.06	-0.25	0.59	0.19				0	2		Y	y	y	y	y
l	12-13	-0.004	0.07	-0.25	0.66	0.18			y	2	2	Y		y	y		y
m	13-14	0.004	-0.07	0.25	0.59	0.20	y			0	3				y		
n	14-15	0.004	-0.06	0.25	0.53	0.22	y			0	2			y	y		
o	15-16	-0.008	0.13	-0.50	0.66	0.17				3	1	Y	Y	y			
p	16-17	0.04	-0.05	0.50	0.61	0.21	y			1	1		Y	y			y
q	17-18	-0.06	-0.01	-0.50	0.6	0.18			y	1	0		Y				
r	18-19	0.04	0.03	0.25	0.63	0.19	y	y		0	2	Y					
s	19-20	-0.02	0.03	-0.25	0.66	0.18			y	2	0	Y					y
t	20-21	0.01	-0.01	0.10	0.65	0.19				1	3			y			y
u	21-22	0.01	-0.02	0.15	0.63	0.21				0	3		Y	y	y		y
v	22-23	-0.01	0.02	-0.15	0.65	0.19				0	3					y	y
w	23-24	-0.01	0.01	-0.10	0.66	0.18				2	2			y			y